Title: Pneumolysin-dependent and independent non-canonical autophagy processes mediate host defense against pneumococcal infection

Authors: Bartosz J. Michno[1,2], Niedharsan Pooranachandran[1], Tonisha C. Smith[3], Erin Faught[4], Sandra Lipowská[1], Andrew K. Fenton[3], Annemarie H. Meijer[4], Tomasz K. Prajsnar[1]

1 Department of Evolutionary Immunology, Institute of Zoology and Biomedical Research, Faculty of Biology, Jagiellonian University, Krakow, Poland

2 Doctoral School of Exact and Natural Sciences, Jagiellonian University, Krakow, Poland

3 School for Biosciences, Florey Institute for Host-Pathogen Interactions, University of Sheffield, Sheffield, United Kingdom

4 Institute of Biology Leiden, Leiden University, Leiden, The Netherlands

Corresponding author: Tomasz K. Prajsnar

Email: tomasz.prajsnar@uj.edu.pl

Phone: +48 12 6645377

Key words:

CASM; LAP; macrophage; *pneumoniae*; STIL; *Streptococcus*; zebrafish

Abstract:

Streptococcus pneumoniae is an opportunistic pathogen responsible for life-threatening diseases including pneumonia and meningitis. The host defense against pneumococci relies heavily on macrophages, which can effectively internalize and degrade bacteria. Recent studies have implicated both canonical and non-canonical autophagy-related processes in bacterial clearance, but the precise pathways mediating defense against *S. pneumoniae* remain unknown. Here, we utilize a well-established zebrafish larval infection model to investigate the role of autophagy in host defense against pneumococci *in vivo*. Using a transgenic autophagy reporter line, we found the autophagy marker Lc3 being recruited to pneumococci-containing vesicles upon bacterial internalization by zebrafish macrophages. The genetic inhibition of core autophagy genes (*atg5* and *atg16l1*) led to loss of the Lc3 associations and their impaired acidification, significantly delaying bacterial clearance. This Lc3 recruitment is partially mediated by LC3-associated phagocytosis (LAP), as knockdown of *cyba* and *rubcn* moderately reduced Lc3 association with phagosomes and diminished pneumococcal degradation. Interestingly, we observed no involvement of xenophagy components in *S. pneumoniae*-infected macrophages, suggesting the activation of another non-canonical autophagy pathway, distinct from LAP, targeting pneumococci-containing phagosomes. Instead, we found that production of pneumococcal pore-forming toxin - pneumolysin induces LAP-independent Lc3 lipidation, which could be abolished by knockdown of *tecpr1a* indicating the involvement of the sphingomyelin-TECPR1-induced LC3 lipidation (STIL) pathway. Collectively, our observations shed new light on the host immune response against *S. pneumoniae*, demonstrating that two distinct non-canonical autophagy pathways mediate bacterial degradation by macrophages and providing potential targets for the development of novel therapies to combat pneumococcal infections.

ABBREVIATIONS: ATG: autophagy related; BMDM: bone marrow-derived macrophage; CASM: conjugation of ATG8 to single membranes; CFU: colony-forming units; Cyba: cytochrome b-245 alpha chain; DPI: diphenyleneiodonium, GFP: green fluorescent protein; hpf: hours post-fertilization; hpi: hours post-infection; LAP: LC3-associated phagocytosis; Map1lc3/Lc3: microtubule-associated protein 1 light chain 3; MEF: mouse embryonic fibroblast; NADPH: Nicotinamide adenine

dinucleotide phosphate; Optn: Optineurin, Ply: pneumolysin; ROS: reactive oxygen species; SLR: sequestosome-like receptors; SQSTM1: Sequestosome 1; STIL: sphingomyelin–TECPR1-induced LC3 lipidation; TECPR1: tectonin β-propeller repeat containing 1.

Introduction

Streptococcus pneumoniae (pneumococcus) is an opportunistic pathogen that colonizes the human upper respiratory tract and is able to invade other tissues including the central nervous system. This bacterium causes several life-threatening diseases such as community-acquired pneumonia (Weiser et al., 2018) resulting in more than 1 million deaths worldwide each year (Ikuta et al., 2022). Pneumococcus has been repeatedly included in the WHO's list of priority bacterial pathogens since 2017 to date (WHO report, 2024). The widespread use of various antibacterial drugs, mostly β-lactam antibiotics such as penicillin or ampicillin, combined with the high genome plasticity of pneumococci facilitates the spread of pneumococcal resistance to drugs and vaccines, limiting their effectiveness (Croucher et al., 2011; van der Poll & Opal, 2009). Therefore, alternative treatment strategies are urgently needed to combat this pathogen.

The first line of defense against invading pneumococci are tissue-resident alveolar macrophages in the lung (Dockrell et al., 2003). Once internalized, the bacteria sequestered in phagosomes are rapidly acidified by activation of vacuolar ATPase (v-ATPase), which pumps protons into the vacuole (Flannagan et al., 2012; Maxson & Grinstein, 2014; Westman & Grinstein, 2021). This acidification is required for *S. pneumoniae* killing by phagocytes in the zebrafish model system (Prajsnar et al., 2022). Furthermore, lysosomal-dependent degradation, following fusion of phagosomes with lysosomes, has been well described in the literature and is known to be involved in the antibacterial response (Kaufmann & Dorhoi, 2016). Aside from classical phagocytosis, other pathways can also lead to intracellular bacteria degradation including autophagy-related mechanisms which are currently being intensively studied (Yuan et al., 2022). These are either canonical pathogen-selective autophagy, also known as xenophagy (Sharma et al., 2018), or more recently identified non-canonical autophagy pathways, collectively referred to as conjugation

of ATG8 to single membranes (CASM) (Durgan & Florey, 2022; Figueras-Novoa et al., 2024).

Xenophagy is a form of canonical autophagy in which either ruptured bacteria-containing phagosomes or pathogens that have escaped into the cytosol are detected and tagged by various proteins such as ubiquitin or glycan-binding galectins (Shaid et al., 2013; Thurston et al., 2012). Subsequently, such labeled bacteria bind to sequestosome-like receptors (SLRs) and microtubule-associated protein 1A/1B light chain 3B (MAP1LC3/LC3) (Galluzzi et al., 2017; Herhaus & Dikic, 2018; Sharma et al., 2018). The LC3 association promotes the phagophore elongation resulting in formation of a double-membrane autophagosome (Melia et al., 2020). It has recently been reported that SLRs such as sequestosome-1 (SQSTM1/p62) and nuclear dot protein 52 kDa (NDP52/CALCOCO2) contribute to the initiation of xenophagy of intracellular *S. pneumoniae* within non-professional phagocytes such as human pulmonary epithelial cells and mouse embryonic fibroblasts (MEFs) *in vitro* (Ogawa et al., 2018, 2020). It has been also shown that pneumolysin (Ply), a pore-forming toxin produced *by S. pneumoniae* that is able to induce membrane rupture of the vesicles containing bacteria leading to subsequent xenophagy (Ogawa et al., 2020).

The most studied non-canonical autophagy pathway is LAP, a form of CASM that involves many of the same molecular components as xenophagy, but not SLRs. In this case, LC3 is recruited to the single-membrane phagosome triggered by perturbation of ionic and pH balance (Durgan & Florey, 2022). It is generally accepted that LC3 lipidation in LAP requires the activity of nicotinamide adenine dinucleotide phosphate (NADPH) oxidase, generating reactive oxygen species (ROS) (Yang et al., 2012). This ROS production has been shown to promote an interaction between v-ATPase and ATG16L1, which initiates the LC3 lipidation (Hooper et al., 2022). We have recently shown that once ROS production is blocked, the LAP response to various bacterial pathogens is greatly reduced (Masud et al., 2019; Prajsnar et al., 2021). In addition, the RUN and cysteine-rich domain containing BECN1/BECLIN1-interacting protein (RUBCN/RUBICON) has been implicated as a positive regulator of LAP acting upstream of NADPH oxidase complex assembly (Yang et al., 2012). Recent *in vitro* evidence has shown that ROS-dependent LAP occurs within mouse bone marrow-derived macrophages (BMDMs) infected by pneumococci and significantly contributes to bacterial degradation (Inomata et al., 2020).

Although the degradation of invading *S. pneumoniae* through LAP or xenophagy has been investigated *in vitro*, results differ between studies in professional and non-professional phagocytes. While in MEFs, xenophagy has been demonstrated to play a role in pneumococcal degradation (Ogawa et al., 2018, 2020), no such response was observed in macrophages (Inomata et al., 2020). Additionally, the specific interplay of these pathways in the wider and more complex host environment have not yet been elucidated. Unveiling the role of these mechanisms *in vivo* would support the development of innovative immunomodulatory approaches against *S. pneumoniae* in the future.

Previously, we established a model of pneumococcal infection in larval zebrafish and described that zebrafish macrophages can prevent dissemination of intravenously administered unencapsulated *S. pneumoniae* (Prajsnar et al., 2022). The macrophages protect infected larvae by internalization and acidification-mediated killing of pneumococci, underscoring the cross-species evolutionary conserved role of these professional phagocytes in host protection against this pathogen, and providing new opportunities to gain insight into the host-pneumococcus interactions *in vivo.*

In the present study, we focus on the role of autophagy-related mechanisms in *S. pneumoniae* infection using zebrafish larvae. We demonstrate that upon internalization of pneumococci, the vast majority of infected macrophages rapidly respond by the Lc3 conjugation to phagosomal membrane which facilitates phagosomal acidification and bacterial killing. We also show that, rather than being mediated by xenophagy, the protective role of autophagy in pneumococcal infection of macrophages is primarily associated with CASM pathways, including LAP and the sphingomyelin–TECPR1-induced LC3 lipidation (STIL) pathway, which is triggered by pneumolysin toxin.

Results

Intracellular *S. pneumoniae* triggers Lc3 recruitment to bacteria-containing phagosomes in zebrafish macrophages.

To determine whether the autophagy response occurs to intracellular pneumococci, we used our previously established *S. pneumoniae* infection model of zebrafish larvae (Prajsnar et al., 2022) using the transgenic zebrafish line *Tg(CMV:EGFP-*

map1lc3b)^{zf155}, hereafter called *CMV:GFP-Lc3* (He et al., 2009). The zebrafish larvae were injected intravenously with fluorescently labeled unencapsulated *S. pneumoniae* (D39 Δ*cps hlpA*::*mKate2*) and the infected larvae fixed at 2, 4 and 7 hour post infection (hpi). Confocal analysis revealed robust activation of the autophagy machinery, as more than 70% of infected phagocytes contained bacterial clusters surrounded by Lc3 at 2 hpi and this response gradually decreased by 7 hpi (Fig. 1A-B). The time-dependent loss of Lc3-bacteria associations is probably associated by rapid autophagic flux associated with degradation of internalized pneumococci that we have observed before (Prajsnar et al., 2022). Indeed, in addition to the decrease of Lc3 associations over time, the distinctive coccus shape of internalized fluorescent bacteria was also lost as a result of subsequent degradation (Fig. 1A). To determine whether this autophagic response is not specific to the capsule-negative D39 Δ*cps* strain, we also analyzed the infection with the parental encapsulated wild-type (D39 WT) *S. pneumoniae* and observed comparable levels of the autophagic machinery activation (Fig. S1A-B). Interestingly, the observed high levels of the Lc3-association response to *S. pneumoniae* infection within zebrafish macrophages contrasts with the response to other Gram-positive bacterium - *Staphylococcus aureus* (Prajsnar et al., 2021), where the Lc3 response occurs less frequently.

Since we have previously shown that the vast majority of unencapsulated pneumococci are internalized by macrophages (Prajsnar et al., 2022), we made an assumption that the observed Lc3-positive infected phagocytes are indeed macrophages. Nevertheless, to confirm the identity of these cells we crossed the *CMV:GFP-Lc3* zebrafish with the *Tg(mpeg1:mCherryF)*^{ump2} transgenic line (hereafter called *mpeg:mCherry-F*), where the membrane-localized mCherry reporter is expressed in zebrafish macrophages (Bernut et al., 2014). The resulting dual transgenic larvae were intravenously infected with Alexa Fluor 647-labelled pneumococci. Microscopic analysis confirmed that the observed phagocytes evoking the Lc3-mediated response to pneumococci are actually macrophages (Fig. 1C). Altogether, these results demonstrate that larval zebrafish serve as a suitable *in vivo* model to study intramacrophage autophagic response to pneumococci.

Genetic inhibition of autophagy impairs pneumococcal killing

Having identified the Lc3 response to *S. pneumoniae*, we subsequently asked whether this process is actively involved in bacterial clearance or helps infected phagocytes to eliminate invading pneumococci by some alternative mechanism.

To this end, using CRISPR-Cas9 we knocked down the autophagy-essential genes: *atg5* and *atg16l1* encoding proteins that facilitate the conjugation of phosphatidylethanolamine to the activated Lc3 (Dikic & Elazar, 2018). The knockdown efficacy was verified by PCR (Fig. S2A-B). We found that the Lc3 signal surrounding the internalized bacteria was greatly reduced (Fig. 2A-B), which indicates that the observed Lc3 associations are indeed the result of an autophagy response to internalized pathogens. Next, the infected control and *atg5 & atg16l1* double knockdown larvae were homogenized and the number of bacteria within individual larvae were enumerated over the course of the infection. We found that although nearly all bacteria were cleared by 20 hpi in both groups, the larvae with impaired autophagy machinery required more time to eliminate the pathogens, especially in the early stages of infection (Fig. 2C). The observation that *S. pneumoniae* clearance is dampened within zebrafish with an impaired autophagic response suggests a host-protective role for the process of Lc3-bacteria association. Previously, we have shown that acidification is required for *S. pneumoniae* killing by phagocytes in the zebrafish model system (Prajsnar et al., 2022). Therefore, in order to determine whether the observed *atg5*/*atg16l1*-dependent autophagic response plays a role in phagosomal acidification, we injected pneumococci pre-stained with a pH-sensitive dye - pHrodo Red into control and autophagy-deficient zebrafish larvae. We observed significantly elevated levels of bacteria within acidic compartments of zebrafish macrophages of control larvae in comparison to the *atg5*/*atg16l1*-depleted counterparts (Fig. 2D-E). Together, these data show that the autophagic response to internalized *S. pneumoniae* enhances the pace of pneumococcal killing by increasing the acidification rate of the bacteria-containing vesicles.

Inhibition of reactive oxygen species (ROS) results in partial reduction of Lc3 associations and impaired bacterial killing

As we observed high levels of Lc3-positive vesicles within pneumococcus-infected macrophages, we sought to elucidate the molecular mechanism responsible for their formation. It is generally accepted that LC3 association with internalized pathogens

can be mediated by either xenophagy or non-canonical autophagic pathways such as LAP. To determine which pathway is primarily responsible in our model, we manipulated phagosomal ROS production, as its inhibition prevents the LAP response in zebrafish to several pathogens (Masud, Prajsnar, et al., 2019; Prajsnar et al., 2021), and recent findings suggest that ROS-dependent LAP is primarily responsible for pneumococcal clearance in BMDMs *in vitro* (Inomata et al., 2020). Using a previously validated morpholino-modified antisense oligonucleotide method (Niethammer et al., 2009), we inhibited the expression of *cyba/p22phox* (cytochrome b-245 alpha chain), a membrane-bound subunit of phagocyte NADPH oxidase. While the morpholino-based targeting of *cyba* was previously shown to effectively inhibit Lc3 assembly on phagosome membranes during infection caused by either Gram-positive or negative bacteria (Masud et al., 2019; Prajsnar et al., 2021, Fig. S1C-D), we surprisingly found that loss of *cyba* resulted in only partial reduction of Lc3 associations (Fig. 3A-B). In agreement with this genetic inactivation, chemical inhibition of NADPH oxidase activity with diphenyleneiodonium (DPI) also showed a similar pattern of incomplete suppression of Lc3 aggregation with internalized pneumococci (Fig. S3). Another protein responsible for LAP is Rubicon, which is part of the class III PI3K complex but also activates the NADPH oxidase promoting LAP (Masud, van der Burg, et al., 2019; Yang et al., 2012). Therefore, we knocked down *rubcn* (the knockdown efficacy was validated by qPCR followed by melt curve analysis for each targeted locus) and observed a significant decrease in Lc3 associations, but again, a large fraction of engulfed pneumococci were sequestered in LC3-positive vesicles (Fig. 3D-E) suggesting the existence of another autophagic pathway. To assess the function of LAP in bacterial killing, we enumerated the bacterial load in control and LAP-deficient infected larvae concentrating at early stages of infection as these timepoints showed significant differences when global autophagy was inhibited (Fig. 2C). Both *cyba* and *rubcn* knockdowns had significantly higher CFU counts at 4 hpi than in control siblings (Fig 3C,F). Taken together, these findings demonstrate that ROS- and Rubcn-dependent LAP occurs in response to pneumococci, plays a host-protective role during infection, but contributes only to a part of the autophagic response to pneumococci in zebrafish macrophages.

Heat-inactivated or pneumolysin-deficient *S. pneumoniae* induce a diminished autophagic response within macrophages

Having established that LAP occurs in response to *S. pneumoniae* infection, we next tested whether the internalized bacterial cells need to be alive, and possibly secreting virulence factors, to induce the observed autophagic response.

First, to determine whether live *S. pneumoniae* cells are required to induce an Lc3-mediated response, larvae were injected with heat-killed bacterial cells. We observed a significant decrease in Lc3 associations with pre-killed bacteria (Fig. 4A-B). Having shown that live pneumococci are required to fully induce the autophagic response in zebrafish macrophages, we speculated whether specific extracellular virulence factors play a role in this process. It has been demonstrated that the induction of the autophagic response to internalized pneumococci by professional and non-professional phagocytes *in vitro* requires Ply (Inomata et al., 2020; Ogawa et al., 2018, 2020). To test whether Ply is responsible for triggering autophagy in zebrafish macrophages, we first generated a *S. pneumoniae* strain in which the *ply* gene has been removed (Δ*ply*) and verified that expression of the Ply protein was not detected by immunoblot (Fig. 4C). We observed significantly less Lc3 associations in phagocytes when *S. pneumoniae* cells lack Ply compared to the control strain (Fig. 4D-E). It is worth noting that both heat-killed and Ply-deficient bacteria were still able to evoke a partial autophagic response (Fig. 4), similar to what we observed in ROS-depleted larvae (Fig. 3). These observations prompted us to perform an experiment where *cyba* morphants were injected with Ply-negative pneumococci. Strikingly, this combination led to virtually complete loss of the Lc3 decoration in pneumococci-infected macrophages (Fig. 4F-G), indicating that pneumolysin induces another autophagic pathway. Overall, our observations confirm the role of pneumolysin in evoking an autophagic response in an *in vivo* system and importantly this pneumolysin-evoked response is independent of LAP.

Lack of xenophagy components does not affect the autophagic response to pneumococci

We considered that xenophagy might be the Ply-mediated autophagy pathway, which complements the ROS-dependent LAP response. During xenophagy, ruptured phagosomes or cytosolic bacteria are detected and labeled with ubiquitin (Manzanillo

et al., 2013; Ogawa et al., 2018; Polajnar et al., 2017; Zhang et al., 2019). Furthermore, the expression of a pore forming toxin, ESAT-6, is required for inducing xenophagy in infection with mycobacteria (Bell et al., 2021). To elucidate whether xenophagy is responsible for the pneumolysin-evoked and LAP-independent Lc3 response, we first sought to detect ubiquitinated bacteria. However, when we performed immunostaining for ubiquitin at 2 hpi, we observed ubiquitin staining in only around 5% of phagocytes containing Lc3-decorated bacteria, suggesting little involvement of pneumococcal ubiquitination within zebrafish phagocytes (Fig. S4).

Next, we took advantage of a previously established double *sqstm1*$^{-/-}$, *optn*$^{-/-}$ mutant zebrafish line, lacking two key SLRs, sequestosome 1 (Sqstm1/p62) and optineurin (Otpn), whose contribution to xenophagy is firmly established and evolutionary conserved (Xie & Meijer, 2023,Gubas & Dikic, 2022). Using the CMV:GFP-Lc3 transgenic background, our confocal analysis revealed a comparable number of Lc3-positive infected phagocyted in the double mutant and wild-type larvae (Fig. 5A-B). Consistently, the kinetics of bacterial clearance remained virtually unchanged in Sqstm1/Optn-deficient larvae when compared to the wild-type siblings (Fig. 5C). We also infected *sqstm1*$^{-/-}$ and *optn*$^{-/-}$ single mutants, and as expected, no differences in Lc3 formation or pneumococcal killing ability was observed (Fig. S5). Next, we reasoned that xenophagy might be triggered within *S. pneumoniae*-infected macrophages under conditions when ROS-dependent LAP is inhibited. To address this possibility, we knocked down *cyba* in *sqstm1*$^{-/-}$ larvae, but found a similar reduction in Lc3 associations within infected phagocytes as those caused by ROS inhibition alone, without any further reductions (Fig. S6).

In order to confirm the lack of xenophagy in pneumococci-infected macrophages, we focused on ATG13, a component of the ULK1 complex that is required for canonical autophagy pathways including xenophagy, but dispensable for LAP (Zachari & Ganley, 2017). Under conditions of *atg13* CRISPR-mediated knockdown (Forn-Cuní et al., 2023), we saw no reduction in Lc3 association with internalized pneumococci in *atg13* knockdown larvae (Fig 5D-E), confirming that the Lc3 response to pneumococci is largely independent of xenophagy.

Overall, these results indicate no apparent role of xenophagy in the autophagic response to pneumococci in zebrafish macrophages suggesting the existence of

another non-canonical autophagic mechanism evoked during the *S. pneumoniae* infection that functions alongside LAP and is triggered by pneumolysin.

A novel *tecpr1a*-mediated pneumolysin-dependent autophagic pathway occurs in pneumococcus-infected macrophages

In pursuit of defining the hypothesized alternative pneumolysin-dependent non-canonical autophagic route (Fig. 4), we speculated that a recently described pathway in the CASM category, called sphingomyelin–TECPR1-induced LC3 lipidation (STIL), could be involved (Figueras-Novoa et al., 2024). This response is triggered upon sphingomyelin translocation from the luminal into the cytosolic leaflet of the phagosomal membrane induced by bacterial toxins such as listeriolysin O, from *Listeria monocytogenes*. It has been postulated that cytosolic sphingomyelin exposure is an early indicator of vesicle damage (Ellison et al., 2020). Importantly, *S. pneumoniae* has been recently shown to induce sphingomyelin exposure to the cytoplasm in phagosomal membranes of infected BMDMs (Shizukuishi et al., 2024). In STIL, the exposed sphingomyelin is recognized by a protein called tectonin β-propeller repeat containing 1 (TECPR1) to induce single membrane LC3 lipidation (Boyle et al., 2023). Interestingly, TECPR1 provides E3-ligase-like activity to the ATG5-ATG12 complex, which is essential for the conjugation of LC3 to damaged phagosomes in the absence of ATG16L1 (Wang et al., 2023). The zebrafish genome contains two paralogues of *TECPR1* called *tecpr1a* and *tecpr1b* (Fig. 6). We performed an alignment of both zebrafish proteins to the human orthologue and we found profoundly higher amino acid similarity between TECPR1 and Tecpr1a in comparison to Tecpr1b, especially within the ATG5-interacting region (AIR) which appears to be incomplete in Tecpr1b (Fig. 6A-B). In addition, using the Zebrafish Blood Atlas web tool with single cell RNAseq gene expression profile of adult zebrafish hematopoietic cells (Athanasiadis et al., 2017), we found that *tecpr1a*, but not *tecpr1b*, is highly expressed in zebrafish leukocytes (Fig. 6C). Based on this analysis, we hypothesized the Tecpr1a variant to be functional in zebrafish, but nevertheless, we knocked down both zebrafish paralogues, *tecpr1a* and *tecpr1b*, using the CRISPR-Cas9 approach and positively-verified their knockdown efficiency (Fig. S2C-D). Interestingly, when challenged by pneumococci, only *tecpr1a* and the *tecpr1a*/*b* double knockdown, but not *tecpr1b* knockdown larvae showed partial reduction of Lc3 decoration within infected macrophages (Fig. 6D-E). This result

suggests that *tecpr1a* is indeed the functional orthologue of human TECPR1, confirming our bioinformatic analysis (Fig. 6A-C). In order to verify the pneumolysin-dependency of the observed *tecpr1a*-mediated Lc3 decoration, we infected the *tecpr1a* knockdown larvae with the pneumolysin-deficient Δ*ply* strain. We found no additive effect in the reduction of Lc3 associations (Fig. 6F-G), indicating both Tecpr1a and Ply act on the same pathway. To provide further evidence for the involvement of the STIL pathway, we checked if the LC3 response to pneumococci would be independent of ATG16l1, which is not required for STIL (Figueras-Novoa et al., 2024; Wang et al., 2023). Knockdown of *atg16l1* resulted in a significant reduction of Lc3 associations. Although some Lc3 signal remained, these results demonstrate the presence of a largely *atg16l1*-independent autophagic response to pneumococci in zebrafish macrophages (Fig. S7), consistent with the requirements of the STIL pathway.

Upon discovery of this novel pathway in pneumococcus-infected macrophages, we set out to determine the role of STIL in pneumococcal killing. The results showed that Tecpr1a-depteted larvae clear the intravenously-administered pneumococci slower than their wild-type siblings. (Fig 6H). Together, these results demonstrate a host-protective role of a non-canonical pathway called STIL that has not been previously been implicated in pneumococcal infection.

Two independently initiated autophagic pathways occur in response to pneumococci

Our data suggests the occurrence of two simultaneous non-canonical autophagic pathways of different nature in response to pneumococci: LAP and STIL, which are both part of the recently recognized and rapidly expanding family of CASM pathways, where LC3/ATG8 is conjugated to single membranes of phagosomes and other organelles (Durgan & Florey, 2022; Figueras-Novoa et al., 2024). In order to confirm the coexistence of these phenomena we knocked down the two specific factors responsible for each of them: *cyba* for LAP and *tecpr1a* for STIL. When both genes were knocked down we observed a near complete loss of Lc3 associations (Fig 7A-B). Notably, this effect of double *cyba* and *tecpr1a* knockdown was substantially pronounced than the partial reductions of Lc3 decorations that we previously observed in separate knockdowns of *cyba* (Fig 3A-B) or *tecpr1a* (Fig. 6 D-E). This

additive effect of *cyba* and *tecpr1a* gene silencing suggests that indeed we observe two separate autophagic pathways evoked in response to internalized pneumococci. Finally, to compare the contributions of LAP and STIL to pneumococcal killing, we determined the level of bacteria in both single and double *cyba tecpr1a* knockdown. This analysis showed that bacteria were killed at a lower pace in larvae where both LAP and STIL were inhibited compared with either of the single knockdown counterparts (Fig. 7C). Collectively, these results confirm the coexistence of LAP and STIL pathways, which both serve host-protective roles and act independently on intracellular pneumococci.

Discussion

Autophagy-related mechanisms, both canonical and non-canonical, are considered to be an important component of host defense against various infections, acting primarily as a protective mechanism, and therefore could be exploited in designing novel therapies (Kimmey & Stallings, 2016). In this study, we aimed to investigate the role of autophagy in the innate immune response to *Streptococcus pneumoniae* systemic infection using a zebrafish larval model. We found that the great majority of infected macrophages contained bacterial clusters surrounded by Lc3 at the early stage of infection (2 hpi) confirming involvement of autophagy in the host response to pneumococci. Importantly, both capsulated and unencapsulated strains, once internalized, were found to effectively activate Lc3 recruitment to pneumococcus-containing vesicles. The LC3 conjugation requires ATG5 which is involved in the covalent attachment of LC3 to the phospholipids of the membrane which is an essential step in the autophagy process (Dikic & Elazar, 2018; Melia et al., 2020). By diminishing the autophagic response through knockdown of *atg5* and *atg16l1*, we observed impaired bacterial clearance in our model. This emphasized the significance of autophagy in facilitating the clearance of intracellular pneumococci by zebrafish macrophages and prompted us to investigate which autophagy-related pathway is responsible for this response. We took a combinatory approach by targeting pathogen and host components, both separately and in combination to determine the autophagic pathways present in *S. pneumoniae*-infected macrophages.

The antimicrobial, host-protective function of LC3-associated phagocytosis (LAP) has been reported in several studies, demonstrating its effective role in bacterial degradation (Grijmans et al., 2022; Herb et al., 2020; Yuan et al., 2022). The significance of this pathway had been recognized well before its inclusion in the recently defined CASM family and it is supported by studies analyzing microbial survival mechanisms evolved to evade or escape this process to prolong their survival (Hubber et al., 2017; Köster et al., 2017; Mitchell et al., 2017). Our study demonstrates that LAP occurs in zebrafish macrophages upon internalizing pneumococci. A significant but partial reduction in Lc3 recruitment and slower bacterial clearance induced by knocking down *cyba* or *rubcn*, genes required for LAP, underscores the importance of this pathway in the host defense against pneumococci. Importantly, our data confirms *in vitro*-derived results where LAP also plays a protective role in pneumococci-infected BMDMs (Inomata et al., 2020). Interestingly, Inomata and colleagues have also reported incomplete inhibition of LC3 recruitment in *Rubcn* or *Nox2* knockout macrophages, which additionally prompted us to search for another autophagic pathway present in response to pneumococci. Moreover, in accordance with Inomata and others, we observed significant decrease of Lc3 associations to pneumococci in the absence of pneumolysin and we did not find any evidence of selective autophagy involvement in *S. pneumoniae*-infected macrophages *in vivo*.

Indeed, our results show that Lc3 recruitment triggered by pneumococci upon internalization by macrophages is partially-dependent on bacterial pneumolysin. By targeting components of different autophagy pathways, we were able to match pathogen-derived pneumolysin with particular facets of the autophagic response. Inomata *et al.* posited that pneumolysin induces LAP, however no combinatory approaches with Δ*ply* mutant in LAP-deficient macrophages have been performed (Inomata et al., 2020). By testing wild-type and Δ*ply* mutant pneumococcal strains against pathway-specific host genes in the zebrafish model, we here show that Ply activates another non-canonical autophagy pathway, which acts independently of ROS and Atg16l1, but is dependent on Tecpr1a.

TECPR1 was initially shown to play a vital role in promoting selective autophagy through interaction with WIPI-2 (Ogawa et al., 2011). However, recent studies have revealed an additional function of TECPR1 via its DysF domains (Boyle et al., 2023;

Kaur et al., 2023), where this protein recognizes sphingomyelin present on the outer layer of disturbed phagosomal or lysosomal membranes to induce CASM in a process called STIL. Interestingly, this alternative non-canonical pathway challenges the traditional view that ATG16L1 is the sole E3-like enzyme responsible for lipidation of LC3, highlighting the versatility and complexity of autophagic regulation (Corkery et al., 2023).

We have found in zebrafish that a knockdown of *tecpr1a*, a likely orthologue of TECPR1, leads to a partial loss of Lc3 decoration of internalized pneumolysin-positive *S. pneumoniae*. When pneumolysin mutant bacteria were administered, no additional effect of *tecpr1a* depletion was observed suggesting the role of pneumolysin in perturbing the phagosomal membrane and Tecpr1a in phagosomal membrane Lc3 decoration. Importantly, in the *cyba tecpr1a* double knockdown we observed a near-complete loss of Lc3 associations. Moreover, in *cyba* knockdown larvae injected with Δ*ply* pneumococci, no Lc3 decoration was present, indicating the occurrence of two independent, differentially induced non-canonical pathways, namely LAP and STIL. A similar phenomenon was previously observed *in vitro* in BMDMs infected with *L. monocytogenes* evoking two distinct non-canonical autophagy pathways (Gluschko et al., 2022). One of them is LAP and the other ROS-independent, listeriolysin O-mediated, was coined by the authors as Pore-Forming toxin-Induced Non-Canonical Autophagy (PINCA). At the time, the authors did not know the factors responsible for PINCA, therefore they were unable to determine its function in *L. monocytogenes* infection. It is conceivable that PINCA observed by Glushko and colleagues was in fact STIL.

Another similar case of two parallel pathways has been observed in MEFs *in vitro* at early stages of infection with pneumolysin-expressing *S. pneumoniae*, where Lc3 lipidation occurred independently of FIP200 (a member of the ULK1 complex required for canonical autophagy) and also independently of ROS leading to LAPosome-like vacuoles formation. However, since the observed process requires ATG16L1 (Ogawa et al., 2020), it appears to be another form of CASM, distinct from STIL. Interestingly, Ogawa and colleagues have reported a hierarchical autophagic response in which LAPosomes undergo Sqstm1- and Optn-mediated xenophagy at later stages of infection (Ogawa et al., 2020; Sakuma et al., 2024). However, no such phenomenon involving xenophagy factors was observed in macrophages, neither in

our study nor in that of others (Inomata et al., 2020). The various mechanisms evoked by pneumococci infection in different cells are most likely caused by differences between professional and non-professional phagocytes, such as the higher levels of ROS production of macrophages compared to fibroblasts or the degree of phagosomal acidification (Inomata et al., 2020).

We propose the following model of the fate of pneumococci within macrophages (Fig. 8). The bacteria are internalized by macrophages and trapped within Lc3-decorated vesicles, which could be formed by two distinct mechanisms depending on the nature of phagosomal membrane perturbation. Florey and others have hypothesized that any process that promotes osmotic imbalances within the endolysosomal system would have the potential to activate LAP-like LC3 lipidation (Florey et al., 2015). Therefore, we believe that in our model, the ROS-induced osmotic imbalance in phagosomes containing pneumococci leads to LAP. Alternatively, pneumolysin produced by bacteria trapped in phagosomes inflicts another form of membrane perturbation, leading to sphingomyelin presence on the outer side of phagosomal envelope and resulting in STIL. This scenario is supported by a recent report demonstrating induction of sphingomyelin exposure to the cytoplasm in phagosomal membranes of *S. pneumoniae*-infected BMDMs (Shizukuishi, Ogawa, & Akeda, 2024). Both LAP and STIL enhance pneumococcal killing within zebrafish macrophages as knockdown of pathway-specific components slowed down the inactivation of bacteria *in vivo*.

It is tempting to speculate that apart from the observed LAP and STIL, there might be another non-canonical autophagy mechanism which is Atg16l1- and Ply-dependent but ROS-independent, as described by Ogawa *et al.* (2020). This possibility could explain why loss of pneumococcal Ply had a bigger impact on Lc3 decoration than inhibition of STIL by Tecpr1a deficiency. Moreover, Atg16l1 depletion had a larger effect than *cyba* knockdown, also suggestive of another ROS-independent pathway contributing the Lc3 response. However, since only the Ply inhibition was achieved by null mutation and the rest of genetic manipulations were knockdowns, our results do not provide conclusive evidence for the presence of a third pathway, and we currently conclude that at least two pathways, LAP and STIL, function in parallel.

Collectively, the presented results markedly advance our knowledge of the innate immune response to pneumococcal infections. By elucidating the abundant activation of LAP and STIL, and probably negligible role of xenophagy in professional phagocytes our study highlights potential therapeutic targets that could be exploited to enhance host defense mechanisms. Therefore, in addition to LAP, we believe it is important to address STIL in order to control pneumococcal infection. This may offer novel ways for treatment, especially in cases where traditional antibiotic-based therapies are insufficient due to rising bacterial resistance, opening the door to innovative immunomodulatory approaches that could improve clinical outcomes in pneumococcal infections.

Materials and Methods

Ethics statement

All zebrafish experiments were conducted in accordance with the European Community Council Directive 2010/63/EU for the Care and Use of Laboratory Animals of Sept. 22, 2010 (Chapter 1, Article 1 no.3) and National Journal of Law act of Jan. 15, 2015, for Protection of animals used for scientific or educational purposes (Chapter 1, Article 2 no.1). All experiments with zebrafish were performed on embryos/larvae up to 56 hours post fertilization and were following ARRIVE guidelines. The Jagiellonian University Zebrafish Core Facility (ZCF) is a licensed breeding and research facility (District Veterinary Inspectorate in Krakow registry; Ministry of Science and Higher Education record no. 022 and 0057).

Zebrafish husbandry

Adult zebrafish were maintained by Zebrafish Core Facility sta□ at the Jagiellonian University in accordance with the standard protocol and international guidelines specified by the EU Animal Protective Directive 2010/63/EU. Fish were kept in a continuous recirculating closed system aquarium with a light/dark cycle of 14/10 hours at 28°C. Larvae were incubated in standard E3 medium at 28.5°C according to standard protocols (Nusslein-Volhard & Dahm, 2002). All zebrafish lines used in this study are listed in Table S1.

Bacterial cultures and infection experiments

All *Streptococcus pneumoniae* strains used in this study were derived from serotype 2 D39 strain (Lanie et al., 2007) and are listed in Table S1. Pneumococci were grown on prepared Tryptic Soy Agar 5% sheep blood plates (TSAII 5% SB; Becton Dickinson) at 37°C in an atmosphere containing 5% CO_2. Liquid cultures were maintained in Todd-Hewitt Broth (Becton-Dickinson) supplemented with 0.5% yeast extract (BD) at 37°C in an atmosphere containing 5% CO_2. Bacteria were harvested at mid-log phase (OD_{600} between 0.2 - 0.3) and subsequently centrifuged (5000 g, 10 min) and immediately resuspended in phosphate-bu□ered saline (PBS) to obtain desired concentration of approximately 1600 CFU/nl. Such prepared bacteria were microinjected intravenously into 36 hpf zebrafish larvae as described previously (Prajsnar et al., 2008). Briefly, larvae were anaesthetized with 0.02% buffered Tricaine (Sigma Aldrich) and then transferred onto 3% w/v methylcellulose (Sigma Aldrich) and injected individually with 1 nl of bacteria inoculum using microcapillary pipettes.

Staining of bacteria with pHrodo-Red and Alexa Fluor 647 S-ester dyes

The pHrodo Red (ThermoFisher) and Alexa Fluor 647 (ThermoFisher) Succinimidyl-ester dyes were dissolved in DMSO (Sigma) to the final concentrations of 2.5 mM and 8 mM, respectively. In indicated experiments, the unlabeled D39 Δ*cps S. pneumoniae* was stained as previously described (Prajsnar et al., 2021).

Generation of Δ*ply* mutant in *S. pneumoniae*

The *S. pneumoniae* Δ*ply* deletion strain was generated using linear PCR fragments. Briefly, two ~1-kb flanking regions of each gene were amplified and an antibiotic resistance marker placed between them using isothermal assembly. Assembled PCR products were transformed directly into *S. pneumoniae*. In all cases, deletion primers were given the typical name: “gene- designation”_5FLANK_F/R for 5′ regions and “gene-designation”_3FLANK_F/R for 3′ regions, antibiotic markers were amplified from Δ*bgaA* strains (Fenton et al., 2016) using the AntibioticMarker_F/R primers. Successful gene deletion strains were confirmed using diagnostic PCR. All bacterial strains and oligonucleotides used in this study are listed in Table S2.

Morpholino- and CRISPR/Cas9-Mediated Knockdown

The *cyba* morpholino oligonucleotides (Niethammer et al., 2009) (Gene Tools) were dissolved in MilliQ water to obtain the required concentrations of 1 mM. The 1 nl volume of morpholino was injected into the yolk of 1–2 cell stage zebrafish embryos using a microinjector. Standard control morpholino (Gene Tools) was used as a negative control. For CRISPR/Cas9-mediated *atg5, atg16l1, rubcn*, *tecpr1a* and *tecpr1b* knockdown, the online web tool CHOPCHOP was used to design a gene-specific guide CRISPR of following sequences listed in Table S3. The synthetic SygRNA (Merck) consisting of gene-specific CRISPR RNA (crRNA) and transactivating RNAs (tracrRNA) in combination with Cas9 nuclease protein (Merck) was used for gene editing. TracrRNA and crRNA were resuspended to a concentration of 50 µM in nuclease-free water. The gRNA-Cas9 complexes were assembled before injections using a 1:1:1 ratio of crRNA:tracrRNA:Cas9 nuclease with the final concentrations of 16.6 µM, 16.6 µM, and 6.6 µM, respectively. As controls, only Cas9 + tracrRNA were injected without crRNA. Knockdown verification was performed by the PCR use of primers with the sequences presented in the Table S2.

DPI treatment

At 1 h before infection, larvae were bath-treated with 100 µM DPI (Sigma Aldrich) in E3 medium. The larvae were then infected and kept in DPI solution until fixation. DMSO at 0.1% was used as vehicle control.

Immunostaining

Larvae were fixed with 4% paraformaldehyde (PFA, ThermoFisher) supplemented with 0.5% Triton X-100 in PBS and incubated overnight at 4°C. Subsequently, fixed fish were washed four times for 20 minutes in PBS with 0.5% Triton-x100 and 1% DMSO (PBS-DTx). Next, the larvae were digested in 10 µg/ml proteinase K (Sigma Aldrich) for 10 minutes at 37°C. Then, larvae were quickly washed three timed for 5 minutes and blocked with PBS-DTx containing 1% bovine serum albumin (BSA) (ThermoFisher) for 1h at room temperature and incubated overnight at 4°C in mono- and polyubiquitinated conjugates recombinant mouse monoclonal antibody (UBCJ2 ; Enzo lifes Siences) diluted in the blocking buffer 1:250. Next, larvae were washed in blocking solution four times for 20 minutes and incubated at room temperature for 2 h

in blocking solution of secondary goat anti-mouse Alexa Fluor 405 antibody (Invitrogen) in 1:300 followed with four times washes in PBS with 0.5% Triton-x100.

Microscopic Imaging and Analysis

Live anaesthetized or PFA-fixed larvae were immersed in 1% (w/v) low-melting-point agarose solution in E3 medium and mounted laterally on a dish with glass bottom. Images were acquired using a Zeiss LSM900 Airyscan 2 confocal laser scanning microscope with ZEISS ZEN 3.3 software using the Plan-Apochromat 20x/0.8, C-Apochromat 40x/NA 1.2 W or C-Apochromat 63x/1.20 W objectives. For quantification of the autophagic response within infected phagocytes, for each larva, a total number of observable infected phagocytes were manually determined through the z-stacks of images. Among these total observable infected phagocytes number of infected phagocytes with GFP-Lc3 signals were enumerated, and the percentage of Lc3-positive phagocytes over total observable phagocytes was determined for each larva. Maximum projections were used for representative images. No non-linear normalization were performed. For quantification of acidification, the pHrodo Red fluorescence intensity, ZEISS ZEN 3.3 software was used.

Determination of *In Vivo* Bacterial Counts

At various times postinfection, approximately 8-12 anesthetized zebrafish larvae were individually transferred with 100 µl of E3 medium into 0.5-ml Screw cap micro tubes (Sarstedt) containing 2-mm Zirconia beads (Biospec) and homogenized using a FastPrep-24 5G homogenizer (MP Biomedicals). The homogenates were spotted on TSA plates containing 5% defibrinated sheep blood to determine pneumococcal CFU numbers. The limit of detection was 10 CFU per larva.

Western Blot

For each immunoblot, 10 µl of each whole-cell lysate was run on a 12% SDS PAGE gel (40 mA, ≈55 min) and transferred onto PVDF membranes (80 min, 50 V). Membranes were blocked with 5% skimmed milk in 1x PBS 0.5% Tween20 for 1 h (gently rocking, room temperature). Membranes were washed three times with 1x PBS, 0.05% Tween20, and incubated with primary antibody overnight gently rocking (4°C, 3% BSA in 1x PBS, 0.05% Tween20, 0.02% sodium azide). For detection of Ply, a mouse anti-Ply antibody was used at a final concentration of 1:1000 (abcam,

Ms mAb to Pneumolysin [PLY-4] AB71810). The blocked PVDF membranes were washed three times with 1x PBS, 0.05% Tween20. The secondary antibody (goat anti-mouse IgG conjugated to horseradish peroxidase [Biorad, Cat #172-1011]) was used at 1:5000 and applied in 1x PBS with 3% BSA for 1 h at room temperature with gentle shaking. Resulting blots were washed four times in 1x PBS, 0.05% Tween20 and visualized using the Clarity Western ECL Substrate kit (BioRad Cat #170-5061) according to the manufacturer's instructions. Blots were imaged using a Syngene G:BOX Chemi XX9 image quantification device combined with the GeneSys software (v1.6.7.0) using the chemiluminescent detection tools.

Statistics

GraphPad Prism 10 was used for statistical analysis. Quantifications of percent Lc3-positive phagocytes or CFU counts were determined for significance with unpaired parametric t-test for 2 groups and with ANOVA for multiple groups, with Šidák correction for multiple comparisons. Statistical significance was assumed at *P*-values below 0.05.

Acknowledgements

This work was supported by a National Science Centre of Poland under Sonata Bis 9 project (Grant number: 2019/34/E/NZ6/00137) awarded to T.K.P. and a Medical Research Council (MRC) New Investigator Research Grant (Grant number: MR/S009280/1) awarded to A.K.F.

T.K.P. was funded by Polish National Agency for Academic Exchange under Polish Returns 2019 project (Grant number: PPN/PPO/2019/1/00029/U/0001) and T.C.S. was funded by MRC DiMeN DTP studentship.

The establishment of Zebrafish Core Facility at the Department of Evolutionary Immunology has been supported by a grant from the Priority Research Area BioS under the Strategic Program Excellence Initiative at Jagiellonian University.

Disclosure statement

The authors have declared no conflict of interests.

References

Athanasiadis, E. I., Botthof, J. G., Andres, H., Ferreira, L., Lio, P., & Cvejic, A. (2017). Single-cell RNA-sequencing uncovers transcriptional states and fate decisions in haematopoiesis. *Nature Communications*, *8*(1). https://doi.org/10.1038/s41467-017-02305-6

Bell, S. L., Lopez, K. L., Cox, J. S., Patrick, K. L., & Watson, R. O. (2021). Galectin-8 senses phagosomal damage and recruits selective autophagy adapter tax1bp1 to control mycobacterium tuberculosis infection in macrophages. *MBio*, *12*(4). https://doi.org/10.1128/mBio.01871-20

Bernut, A., Herrmann, J. L., Kissa, K., Dubremetz, J. F., Gaillard, J. L., Lutfalla, G., & Kremer, L. (2014). Mycobacterium abscessus cording prevents phagocytosis and promotes abscess formation. *Proceedings of the National Academy of Sciences of the United States of America*, *111*(10). https://doi.org/10.1073/pnas.1321390111

Boyle, K. B., Ellison, C. J., Elliott, P. R., Schuschnig, M., Grimes, K., Dionne, M. S., Sasakawa, C., Munro, S., Martens, S., & Randow, F. (2023). TECPR1 conjugates LC3 to damaged endomembranes upon detection of sphingomyelin exposure . *The EMBO Journal*, *42*(17). https://doi.org/10.15252/embj.2022113012

Corkery, D. P., Castro-Gonzalez, S., Knyazeva, A., Herzog, L. K., & Wu, Y. (2023). An ATG12-ATG5-TECPR1 E3-like complex regulates unconventional LC3 lipidation at damaged lysosomes. *EMBO Reports*, *24*(9). https://doi.org/10.15252/embr.202356841

Croucher, N. J., Harris, S. R., Fraser, C., Quail, M. A., Burton, J., Van Der Linden, M., McGee, L., Von Gottberg, A., Song, J. H., Ko, K. S., Pichon, B., Baker, S., Parry, C. M., Lambertsen, L. M., Shahinas, D., Pillai, D. R., Mitchell, T. J., Dougan, G., Tomasz, A., … Bentley, S. D. (2011). Rapid pneumococcal evolution in response to clinical interventions. *Science*, *331*(6016), 430–434. https://doi.org/10.1126/science.1198545

Dikic, I., & Elazar, Z. (2018). Mechanism and medical implications of mammalian autophagy. In *Nature Reviews Molecular Cell Biology* (Vol. 19, Issue 6, pp. 349–364). Nature Publishing Group. https://doi.org/10.1038/s41580-018-0003-4

Dockrell, D. H., Marriott, H. M., Prince, L. R., Ridger, V. C., Ince, P. G., Hellewell, P. G., & Whyte, M. K. B. (2003). Alveolar Macrophage Apoptosis Contributes to

Pneumococcal Clearance in a Resolving Model of Pulmonary Infection. *The Journal of Immunology*, *171*(10), 5380–5388. https://doi.org/10.4049/jimmunol.171.10.5380

Durgan, J., & Florey, O. (2022). Many roads lead to CASM: Diverse stimuli of noncanonical autophagy share a unifying molecular mechanism. In *Science Advances* (Vol. 8, Issue 43). Sci Adv. https://doi.org/10.1126/sciadv.abo1274

Ellison, C. J., Kukulski, W., Boyle, K. B., Munro, S., & Randow, F. (2020). Transbilayer Movement of Sphingomyelin Precedes Catastrophic Breakage of Enterobacteria-Containing Vacuoles. *Current Biology*, *30*(15), 2974-2983.e6. https://doi.org/10.1016/j.cub.2020.05.083

Fenton, A. K., Mortaji, L. El, Lau, D. T. C., Rudner, D. Z., & Bernhardt, T. G. (2016). CozE is a member of the MreCD complex that directs cell elongation in Streptococcus pneumoniae. *Nature Microbiology*, *2*. https://doi.org/10.1038/nmicrobiol.2016.237

Figueras-Novoa, C., Timimi, L., Marcassa, E., Ulferts, R., & Beale, R. (2024). Conjugation of ATG8s to single membranes at a glance. *Journal of Cell Science*, *137*(15). https://doi.org/10.1242/jcs.261031

Flannagan, R. S., Jaumouillé, V., & Grinstein, S. (2012). The cell biology of phagocytosis. In *Annual Review of Pathology: Mechanisms of Disease* (Vol. 7, pp. 61–98). https://doi.org/10.1146/annurev-pathol-011811-132445

Florey, O., Gammoh, N., Kim, S. E., Jiang, X., & Overholtzer, M. (2015). V-ATPase and osmotic imbalances activate endolysosomal LC3 lipidation. *Autophagy*, *11*(1), 88–99. https://doi.org/10.4161/15548627.2014.984277

Forn-Cuní, G., Welvaarts, L., Stel, F. M., van den Hondel, C. J., Arentshorst, M., Ram, A. F. J., & Meijer, A. H. (2023). Stimulating the autophagic-lysosomal axis enhances host defense against fungal infection in a zebrafish model of invasive Aspergillosis. *Autophagy*, *19*(1), 324–337. https://doi.org/10.1080/15548627.2022.2090727

Galluzzi, L., Baehrecke, E. H., Ballabio, A., Boya, P., Bravo-San Pedro, J. M., Cecconi, F., Choi, A. M., Chu, C. T., Codogno, P., Colombo, M. I., Cuervo, A. M., Debnath, J., Deretic, V., Dikic, I., Eskelinen, E., Fimia, G. M., Fulda, S., Gewirtz, D. A., Green, D. R., … Kroemer, G. (2017). Molecular definitions of autophagy and related processes. *The EMBO Journal*, *36*(13), 1811–1836. https://doi.org/10.15252/embj.201796697

Gluschko, A., Farid, A., Herb, M., Grumme, D., Krönke, M., & Schramm, M. (2022). Macrophages target Listeria monocytogenes by two discrete non-canonical autophagy pathways. *Autophagy*, *18*(5), 1090–1107. https://doi.org/10.1080/15548627.2021.1969765

Grijmans, B. J. M., van der Kooij, S. B., Varela, M., & Meijer, A. H. (2022). LAPped in Proof: LC3-Associated Phagocytosis and the Arms Race Against Bacterial Pathogens. In *Frontiers in Cellular and Infection Microbiology* (Vol. 11). Frontiers Media S.A. https://doi.org/10.3389/fcimb.2021.809121

Gubas, A., & Dikic, I. (2022). A guide to the regulation of selective autophagy receptors. *FEBS Journal*, *289*(1), 75–89. https://doi.org/10.1111/febs.15824

He, C., Bartholomew, C. R., Zhou, W., & Klionsky, D. J. (2009). Assaying autophagic activity in transgenic GFP-Lc3 and GFP-Gabarap zebrafish embryos. *Autophagy*, *5*(4), 520–526. https://doi.org/10.4161/auto.5.4.7768

Herb, M., Gluschko, A., & Schramm, M. (2020). LC3-associated phagocytosis - The highway to hell for phagocytosed microbes. In *Seminars in Cell and Developmental Biology* (Vol. 101, pp. 68–76). Elsevier Ltd. https://doi.org/10.1016/j.semcdb.2019.04.016

Herhaus, L., & Dikic, I. (2018). Regulation of Salmonella-host cell interactions via the ubiquitin system. In *International Journal of Medical Microbiology* (Vol. 308, Issue 1, pp. 176–184). Elsevier GmbH. https://doi.org/10.1016/j.ijmm.2017.11.003

Hooper, K. M., Jacquin, E., Li, T., Goodwin, J. M., Brumell, J. H., Durgan, J., & Florey, O. (2022). V-ATPase is a universal regulator of LC3-associated phagocytosis and non-canonical autophagy. *Journal of Cell Biology*, *221*(6). https://doi.org/10.1083/jcb.202105112

Hubber, A., Kubori, T., Coban, C., Matsuzawa, T., Ogawa, M., Kawabata, T., Yoshimori, T., & Nagai, H. (2017). Bacterial secretion system skews the fate of Legionella-containing vacuoles towards LC3-associated phagocytosis. *Scientific Reports*, *7*. https://doi.org/10.1038/srep44795

Ikuta, K. S., Swetschinski, L. R., Aguilar, G. R., Sharara, F., Mestrovic, T., Gray, A. P., Weaver, N. D., Wool, E. E., Han, C., Hayoon, A. G., Aali, A., Abate, S. M., Abbasi-Kangevari, M., Abbasi-Kangevari, Z., Abd-Elsalam, S., Abebe, G., Abedi, A., Abhari, A. P., Abidi, H., … Naghavi, M. (2022). Global mortality associated with 33 bacterial pathogens in 2019: a systematic analysis for the Global Burden

of Disease Study 2019. *The Lancet*, *400*(10369), 2221–2248. https://doi.org/10.1016/S0140-6736(22)02185-7

Inomata, M., Xu, S., Chandra, P., Meydani, S. N., Takemura, G., Philips, J. A., & Leong, J. M. (2020). Macrophage LC3-associated phagocytosis is an immune defense against Streptococcus pneumoniae that diminishes with host aging. *Proceedings of the National Academy of Sciences of the United States of America*, *117*(52). https://doi.org/10.1073/PNAS.2015368117

Kaufmann, S. H. E., & Dorhoi, A. (2016). Molecular Determinants in Phagocyte-Bacteria Interactions. In *Immunity* (Vol. 44, Issue 3, pp. 476–491). Cell Press. https://doi.org/10.1016/j.immuni.2016.02.014

Kaur, N., de la Ballina, L. R., Haukaas, H. S., Torgersen, M. L., Radulovic, M., Munson, M. J., Sabirsh, A., Stenmark, H., Simonsen, A., Carlsson, S. R., & Lystad, A. H. (2023). TECPR1 is activated by damage-induced sphingomyelin exposure to mediate noncanonical autophagy . *The EMBO Journal*, *42*(17). https://doi.org/10.15252/embj.2022113105

Kimmey, J. M., & Stallings, C. L. (2016). Bacterial Pathogens versus Autophagy: Implications for Therapeutic Interventions. In *Trends in Molecular Medicine* (Vol. 22, Issue 12, pp. 1060–1076). Trends Mol Med. https://doi.org/10.1016/j.molmed.2016.10.008

Köster, S., Upadhyay, S., Chandra, P., Papavinasasundaram, K., Yang, G., Hassan, A., Grigsby, S. J., Mittal, E., Park, H. S., Jones, V., Hsu, F. F., Jackson, M., Sassetti, C. M., & Philips, J. A. (2017). Mycobacterium tuberculosis is protected from NADPH oxidase and LC3-associated phagocytosis by the LCP protein CpsA. In *Proceedings of the National Academy of Sciences of the United States of America* (Vol. 114, Issue 41, pp. E8711–E8720). National Academy of Sciences. https://doi.org/10.1073/pnas.1707792114

Lanie, J. A., Ng, W. L., Kazmierczak, K. M., Andrzejewski, T. M., Davidsen, T. M., Wayne, K. J., Tettelin, H., Glass, J. I., & Winkler, M. E. (2007). Genome sequence of Avery's virulent serotype 2 strain D39 of Streptococcus pneumoniae and comparison with that of unencapsulated laboratory strain R6. *Journal of Bacteriology*, *189*(1), 38–51. https://doi.org/10.1128/JB.01148-06

Manzanillo, P. S., Ayres, J. S., Watson, R. O., Collins, A. C., Souza, G., Rae, C. S., Schneider, D. S., Nakamura, K., Shiloh, M. U., & Cox, J. S. (2013). The ubiquitin ligase parkin mediates resistance to intracellular pathogens. *Nature*, *501*(7468),

512–516. https://doi.org/10.1038/nature12566

Masud, S., Prajsnar, T. K., Torraca, V., Lamers, G. E. M., Benning, M., Van Der Vaart, M., & Meijer, A. H. (2019). Macrophages target Salmonella by Lc3-associated phagocytosis in a systemic infection model. *Autophagy*, *15*(5), 796–812. https://doi.org/10.1080/15548627.2019.1569297

Masud, S., van der Burg, L., Storm, L., Prajsnar, T. K., & Meijer, A. H. (2019). Rubicon-Dependent Lc3 Recruitment to Salmonella-Containing Phagosomes Is a Host Defense Mechanism Triggered Independently From Major Bacterial Virulence Factors. *Frontiers in Cellular and Infection Microbiology*, *9*. https://doi.org/10.3389/fcimb.2019.00279

Maxson, M. E., & Grinstein, S. (2014). The vacuolar-type H+-ATPase at a glance - more than a proton pump. *Journal of Cell Science*, *127*(23), 4987–4993. https://doi.org/10.1242/jcs.158550

Melia, T. J., Lystad, A. H., & Simonsen, A. (2020). Autophagosome biogenesis: From membrane growth to closure. In *Journal of Cell Biology* (Vol. 219, Issue 6). Rockefeller University Press. https://doi.org/10.1083/JCB.202002085

Mitchell, G., Cheng, M. I., Chen, C., Nguyen, B. N., Whiteley, A. T., Kianian, S., Cox, J. S., Green, D. R., McDonald, K. L., & Portnoy, D. A. (2017). Listeria monocytogenes triggers noncanonical autophagy upon phagocytosis, but avoids subsequent growth-restricting xenophagy. *Proceedings of the National Academy of Sciences of the United States of America*, *115*(2), E210–E217. https://doi.org/10.1073/pnas.1716055115

Niethammer, P., Grabher, C., Look, A. T., & Mitchison, T. J. (2009). A tissue-scale gradient of hydrogen peroxide mediates rapid wound detection in zebrafish. *Nature*, *459*(7249), 996–999. https://doi.org/10.1038/nature08119

Nusslein-Volhard, C., & Dahm, R. (2002). *Zebrafish: A Practical Approach*. Oxford University Press; Illustrated Edition (November 21, 2002). https://global.oup.com/academic/product/zebrafish-9780199638086

Ogawa, M., Matsuda, R., Takada, N., Tomokiyo, M., Yamamoto, S., Shizukusihi, S., Yamaji, T., Yoshikawa, Y., Yoshida, M., Tanida, I., Koike, M., Murai, M., Morita, H., Takeyama, H., Ryo, A., Guan, J. L., Yamamoto, M., Inoue, J. ichiro, Yanagawa, T., … Ohnishi, M. (2018). Molecular mechanisms of Streptococcus pneumoniae-targeted autophagy via pneumolysin, Golgi-resident Rab41, and Nedd4-1-mediated K63-linked ubiquitination. *Cellular Microbiology*, *20*(8).

https://doi.org/10.1111/cmi.12846

Ogawa, M., Takada, N., Shizukuishi, S., Tomokiyo, M., Chang, B., Yoshida, M., Kakuta, S., Tanida, I., Ryo, A., Guan, J. L., Takeyama, H., & Ohnishi, M. (2020). Streptococcus pneumoniae triggers hierarchical autophagy through reprogramming of LAPosome-like vesicles via NDP52-delocalization. *Communications Biology*, *3*(1). https://doi.org/10.1038/s42003-020-0753-3

Ogawa, M., Yoshikawa, Y., Kobayashi, T., Mimuro, H., Fukumatsu, M., Kiga, K., Piao, Z., Ashida, H., Yoshida, M., Kakuta, S., Koyama, T., Goto, Y., Nagatake, T., Nagai, S., Kiyono, H., Kawalec, M., Reichhart, J. M., & Sasakawa, C. (2011). A Tecpr1-dependent selective autophagy pathway targets bacterial pathogens. *Cell Host and Microbe*, *9*(5), 376–389. https://doi.org/10.1016/j.chom.2011.04.010

Polajnar, M., Dietz, M. S., Heilemann, M., & Behrends, C. (2017). Expanding the host cell ubiquitylation machinery targeting cytosolic Salmonella . *EMBO Reports*, *18*(9), 1572–1585. https://doi.org/10.15252/embr.201643851

Prajsnar, T. K., Cunliffe, V. T., Foster, S. J., & Renshaw, S. A. (2008). A novel vertebrate model of Staphylococcus aureus infection reveals phagocyte-dependent resistance of zebrafish to non-host specialized pathogens. *Cellular Microbiology*, *10*(11), 2312–2325. https://doi.org/10.1111/j.1462-5822.2008.01213.x

Prajsnar, T. K., Michno, B. J., Pooranachandran, N., Fenton, A. K., Mitchell, T. J., Dockrell, D. H., & Renshaw, S. A. (2022). Phagosomal Acidification Is Required to Kill Streptococcus pneumoniae in a Zebrafish Model. *Cellular Microbiology*, *2022*. https://doi.org/10.1155/2022/9429516

Prajsnar, T. K., Serba, J. J., Dekker, B. M., Gibson, J. F., Masud, S., Fleming, A., Johnston, S. A., Renshaw, S. A., & Meijer, A. H. (2021). The autophagic response to Staphylococcus aureus provides an intracellular niche in neutrophils. *Autophagy*, *17*(4), 888–902. https://doi.org/10.1080/15548627.2020.1739443

Sakuma, C., Shizukuishi, S., Ogawa, M., Honjo, Y., Takeyama, H., Guan, J. L., Weiser, J., Sasai, M., Yamamoto, M., Ohnishi, M., & Akeda, Y. (2024). Individual Atg8 paralogs and a bacterial metabolite sequentially promote hierarchical CASM-xenophagy induction and transition. *Cell Reports*, *43*(5). https://doi.org/10.1016/j.celrep.2024.114131

Shaid, S., Brandts, C. H., Serve, H., & Dikic, I. (2013). Ubiquitination and selective autophagy. In *Cell Death and Differentiation* (Vol. 20, Issue 1, pp. 21–30). https://doi.org/10.1038/cdd.2012.72

Sharma, V., Verma, S., Seranova, E., Sarkar, S., & Kumar, D. (2018). Selective autophagy and xenophagy in infection and disease. In *Frontiers in Cell and Developmental Biology* (Vol. 6, Issue NOV). Front Cell Dev Biol. https://doi.org/10.3389/fcell.2018.00147

Shizukuishi, S., Ogawa, M., & Akeda, Y. (2024). Individual Atg8 paralogs exhibit unique properties in streptococcus pneumoniae-induced hierarchical autophagy. In *Autophagy*. Taylor and Francis Ltd. https://doi.org/10.1080/15548627.2024.2375707

Shizukuishi, S., Ogawa, M., Kuroda, E., Hamaguchi, S., Sakuma, C., Kakuta, S., Tanida, I., Uchiyama, Y., Akeda, Y., Ryo, A., & Ohnishi, M. (2024). Pneumococcal sialidase promotes bacterial survival by fine-tuning of pneumolysin-mediated membrane disruption. *Cell Reports*, *43*(3), 113962. https://doi.org/10.1016/j.celrep.2024.113962

Thurston, T. L. M., Wandel, M. P., Von Muhlinen, N., Foeglein, Á., & Randow, F. (2012). Galectin 8 targets damaged vesicles for autophagy to defend cells against bacterial invasion. *Nature*, *482*(7385), 414–418. https://doi.org/10.1038/nature10744

van der Poll, T., & Opal, S. M. (2009). Pathogenesis, treatment, and prevention of pneumococcal pneumonia. In *The Lancet* (Vol. 374, Issue 9700, pp. 1543–1556). Elsevier B.V. https://doi.org/10.1016/S0140-6736(09)61114-4

Wang, Y., Jefferson, M., Whelband, M., Kreuzer, K., Mccoll, J., Verkade, P., Mayer, U., & Wileman, T. (2023). TECPR1 provides E3-ligase like activity to the ATG5-ATG12 complex to conjugate LC3/ATG8 to damaged lysosomes. *BioRxiv*, 2023.06.24.546289. https://doi.org/10.1101/2023.06.24.546289

Weiser, J. N., Ferreira, D. M., & Paton, J. C. (2018). Streptococcus pneumoniae: Transmission, colonization and invasion. In *Nature Reviews Microbiology* (Vol. 16, Issue 6, pp. 355–367). Nature Publishing Group. https://doi.org/10.1038/s41579-018-0001-8

Westman, J., & Grinstein, S. (2021). Determinants of Phagosomal pH During Host-Pathogen Interactions. In *Frontiers in Cell and Developmental Biology* (Vol. 8). Frontiers Media S.A. https://doi.org/10.3389/fcell.2020.624958

Xie, J., & Meijer, A. H. (2023). Xenophagy receptors Optn and p62 and autophagy modulator Dram1 independently promote the zebrafish host defense against Mycobacterium marinum. *Frontiers in Cellular and Infection Microbiology*, *13*. https://doi.org/10.3389/fcimb.2023.1331818

Yang, C. S., Lee, J. S., Rodgers, M., Min, C. K., Lee, J. Y., Kim, H. J., Lee, K. H., Kim, C. J., Oh, B., Zandi, E., Yue, Z., Kramnik, I., Liang, C., & Jung, J. U. (2012). Autophagy protein rubicon mediates phagocytic NADPH oxidase activation in response to microbial infection or TLR stimulation. *Cell Host and Microbe*, *11*(3), 264–276. https://doi.org/10.1016/j.chom.2012.01.018

Yuan, J., Zhang, Q., Chen, S., Yan, M., & Yue, L. (2022). LC3-Associated Phagocytosis in Bacterial Infection. In *Pathogens* (Vol. 11, Issue 8). MDPI. https://doi.org/10.3390/pathogens11080863

Zachari, M., & Ganley, I. G. (2017). The mammalian ULK1 complex and autophagy initiation. *Essays in Biochemistry*, *61*(6), 585. https://doi.org/10.1042/EBC20170021

Zhang, R., Varela, M., Vallentgoed, W., Forn-Cuni, G., van der Vaart, M., & Meijer, A. H. (2019). The selective autophagy receptors Optineurin and p62 are both required for zebrafish host resistance to mycobacterial infection. *PLoS Pathogens*, *15*(2). https://doi.org/10.1371/journal.ppat.1007329

Figure Legends

Figure 1. The autophagic response occurs during systemic infection with pneumococci

A) representative confocal images of *CMV:GFP-Lc3* larvae infected systemically with approximately 1600 CFU of mKate2-labeled D39 Δ*cps S. pneumoniae* and fixed at 2, 4 and 7 hpi. Scale bars: 10 µm. **B**) Quantification of Lc3 associations with intracellular *S. pneumoniae* within infected phagocytes of fixed *CMV:GFP-Lc3* at 2, 4 and 7 hpi. Data are shown as mean ± standard deviation (SD). Data obtained from two independent experiments **C**) representative confocal images of *CMV:GFP-Lc3 mpeg:mCherry-F* dual transgenic larvae infected systemically with approximately 1600 CFU of Alexa Fluor 647-stained D39 Δ*cps S. pneumoniae* and fixed at 2 hpi.

Figure 2. The autophagic response contributes to phagosomal acidification and pneumococcal clearance

A) representative confocal images of control (left panel) and *atg5*, *atg16l1* double knock-down (right panel) CMV:GFP-Lc3 larvae infected systemically with approximately 1600 CFU of mKate2-labeled D39 Δ*cps S. pneumoniae* and fixed at 2 hpi. Scale bars: 10 µm. **B**) Quantification of Lc3 associations with intracellular bacteria of control and *atg5* and *atg16l1* double knock-down larvae. Data are shown as individual values ± standard deviation (SD). Data obtained from two independent experiments. **C**) Numbers of viable colony forming units (CFUs) control or *atg5*, *atg16l1* knockdown larvae infected intravenously with approximately 1600 CFU of *S. pneumoniae* monitored at 2, 4, 7 and 20 hpi. Data obtained from two independent experiments **D**) Representative *in vivo* images of circulation valley of control (top) and *atg5*, *atg16l1* knockdown larvae (bottom) at 2 hpi injected with *S. pneumoniae* D39 Δ*cps* prestained with pHrodo Red. Panels on the right represent zoomed-in areas (indicated by dashed squares). Scale bars represent 10 µm . **E**) Quantification of pHrodo Red fluorescence intensity within phagocytes containing pneumococci. Data obtained from two independent experiments). *** - $p<0.001$.

Figure 3. ROS-dependent autophagic response contribute to clearance of *S. pneumoniae*

A, D) representative confocal images of control and indicated gene knockdown (A – *cyba*, D - *rubcn*) CMV:GFP-Lc3 larvae infected systemically with approximately 1600 CFU of mKate2-labeled D39 Δ*cps S. pneumoniae* and fixed at 2 hpi. Scale bars: 10 µm. **B, E**) Quantification of Lc3 associations with intracellular *S. pneumoniae* within infected phagocytes of fixed CMV:GFP-Lc3 control and indicated gene knockdown (B – *cyba*, E - *rubcn*) larvae at 2 hpi. Data are shown as mean ± standard deviation (SD). Data obtained from three independent experiments. **C, F**) Numbers of viable colony forming units (CFUs) over time of control and indicated gene knockdown (C – *cyba*, F - *rubcn*). Data obtained from three independent experiments.

Figure 4. Live and pnemolysin-positive pneumococci are required to fully induce Lc3-mediated response within zebrafish macrophages

A) representative confocal images of CMV:GFP-Lc3 larvae infected systemically with approximately 1600 CFU of live (left panel) and heat-killed (right panel) mKate2-labeled D39 Δ*cps S. pneumoniae* fixed at 2 hpi. Scale bars: 10 µm. **B**) Quantification of Lc3 associations with intracellular alive or heat-killed *S. pneumoniae* within infected phagocytes of fixed CMV:GFP-Lc3 larvae at 2 hpi. Data are shown as mean ± standard deviation (SD). Data obtained from two independent experiments. **C**) Anti-Ply immunoblot analysis of whole-cell lysates from the indicated *S. pneumoniae* strains. The position of protein markers are indicated in kiloDaltons, Pneumolysin (Ply) ≈ 53.7 KDa. Representative blot shown, n = 4. **D**) representative confocal images of control CMV:GFP-Lc3 larvae infected systemically with approximately 1600 CFU of Ply-positive (D39 Δ*cps*, left panel) and Ply-negative (D39 Δ*cps* Δ*ply*, right panel) mKate2-labeled *S. pneumoniae* fixed at 2 hpi. Scale bars: 10 µm. **E**) Quantification of Lc3 associations with intracellular Ply-positive or Ply-negative *S. pneumoniae* within infected phagocytes of fixed CMV:GFP-Lc3 larvae at 2 hpi. Data are shown as mean ± standard deviation (SD). Data obtained from two independent experiments.

Figure 5. Sqstm1, optineurin and atg13 are not involved in autophagic response to *S. pneumoniae*

A) representative confocal images of *sqstm1* $^{+/+}$/*optn*$^{+/+}$ and *sqstm1* $^{-/-}$/*optn*$^{-/-}$ double mutant (right panel) CMV:GFP-Lc3 larvae infected systemically with approximately 1600 CFU of mKate2-labeled D39 Δ*cps S. pneumoniae* and fixed at 2 hpi Scale bars: 10 µm. **B**) Quantification of Lc3 associations with intracellular *S. pneumoniae* within

infected phagocytes of fixed CMV:GFP-Lc3 *sqstm1* $^{+/+}$/*optn*$^{+/+}$ and *sqstm1* $^{-/-}$/*optn*$^{-/-}$ double mutant larvae. Data are shown as mean ± standard deviation (SD). Data obtained from two independent experiments. **C**) Numbers of viable colony forming units (CFUs) over time of *sqstm1* $^{+/+}$/*optn*$^{+/+}$ and *sqstm1* $^{-/-}$ and *sqstm1* $^{-/-}$/*optn*$^{-/-}$ double mutant larvae. Data obtained from two independent experiments. **D**) representative confocal images of control and *atg13* knockdown (right panel) CMV:GFP-Lc3 larvae infected systemically with approximately 1600 CFU of mKate2-labeled D39 Δ*cps S. pneumoniae* and fixed at 2 hpi Scale bars: 10 µm. **E**) Quantification of Lc3 associations with intracellular *S. pneumoniae* within infected phagocytes of fixed CMV:GFP-Lc3 control and *atg13* knockdown larvae. Data are shown as mean ± standard deviation (SD). n≥15 zebrafish larvae were analyzed.

Figure 6. Tecpr1a, a likely ortholog of human TECPR1, controls Ply-mediated autophagic response to pneumococci

A) Table summarizing the alignment of zebrafish Tecpr1a and Tecpr1b proteins to the human TECPR1 protein. Columns display percentage positives (identical amino acids, as well as conserved or semiconserved substitutions) and length of the proteins. Alignments sequence similarities are shown for the full-length protein and the AIR domain, which exhibits the greatest divergence between the zebrafish paralogues (Tecpr1a and Tecpr1b). **B**) Schematic representation of zebrafish Tecpr1a and Tecpr1b proteins, showing their domains: DysF - Dysferlin, AIR - ATG5-interacting region, and PH - Pleckstrin homology domain. Alignment of the AIR domain amino acid sequence of Human TECPR1 and the zebfafish orthologs, Tecpr1a and Tecpr1b, is shown between the schematics. Symbols denote: (*) identical residues, (:) conserved substitutions, and (.) semiconserved substitutions. **C)** Gene expression of adult zebrafish leukocytes determined using the Zebrafish Blood Atlas (Athanasiadis et al., 2017). Each dot represents a separate scRNAseq sample (cell); replicates were performed across multiple zebrafish wild-type and transgenic strains. Each arm of the schematic represents a separate blood cell population (labeled). Deeper color indicates higher expression (log_{10} scale bars described for each gene). **D**) representative confocal images of control, *tecpr1a*, *tecpr1b* and *tecpr1a*/*b* double knockdown CMV:GFP-Lc3 larvae infected systemically with approximately 1600 CFU of mKate2-labeled D39 *Δcps S. pneumoniae* fixed at 2 hpi. **E**) Quantification of Lc3 associations with intracellular *S. pneumoniae* within

infected phagocytes of fixed tecpr1a, tecpr1b and tecpr1a/b double knockdown CMV:GFP-Lc3 larvae. Data are shown as mean ± standard deviation (SD). n≥17 zebrafish larvae were analyzed. **F**) representative confocal images of control or *tecpr1a* knockdown CMV:GFP-Lc3 larvae infected systemically with approximately 1600 CFU of mKate2-labeled Ply-positive (D39 Δ*cps*) or Ply-negative (D39 Δ*cps* Δ*ply*) *S. pneumoniae* fixed at 2 hpi. **G**) Quantification of Lc3 associations with intracellular Ply-positive or Ply-negative *S. pneumoniae* within infected phagocytes of control or *tecpr1a* knockdown CMV:GFP-Lc3 larvae fixed at 2 hpi. Data are shown as mean ± standard deviation (SD). Data obtained from two independent experiments. **H**) Numbers of viable colony forming units (CFUs) over time of control and *tecpr1a* knockdown larvae. Data obtained from two independent experiments.

Figure 7. Both LAP and STIL are evoked in response to *S. pneumoniae*

A) representative confocal images of control, *cyba, tecpr1a* and *cyba*/*tecpr1a* double knockdown CMV:GFP-Lc3 larvae infected systemically with approximately 1600 CFU of mKate2-labeled D39 *Δcps S. pneumoniae* fixed at 2 hpi. **B**) Quantification of Lc3 associations with intracellular *S. pneumoniae* within infected phagocytes of fixed *cyba, tecpr1a* and *cyba*/*tecpr1a* double knockdown CMV:GFP-Lc3 larvae. Data are shown as mean ± standard deviation (SD). Data obtained from two independent experiments. **C**) Numbers of viable colony forming units (CFUs) over time of control, *cyba*, *tecpr1a and cyba*/*tecpr1a* double knockdown larvae. Data obtained from two independent experiments.

Figure 8. Model of *S. pneumoniae* autophagic response to pneumococci within zebrafish macrophages

After internalisation by phagocytes, pneumococci are sequestered within Lc3-decorated vacuoles which are formed by two independent mechanisms: ROS-dependent LAP or Ply-mediated STIL. LAP occurs as a result of osmotic imbalance within bacteria-containing phagosome as a result of ROS production by NADPH oxidase. On the other hand, STIL is induced upon membrane perturbation caused by secretion of bacterial pneumolysin manifested by sphingomyelin presence on the outside leaflet of the phagosome. STIL is dependent on Tecpr1a which recognizes sphingomyelin and mediates Lc3 lipidation. Following Lc3-assisted vacuolar sequestration, pneumococci are more efficiently targeted for lysosomal degradation

and the Lc3 decoration is removed. The classical xenophagy receptors (sqstm1 and optineurin) as well as the canonical autophagy initiation molecule (atg13) are dispensable in this model. Despite the absence of these xenophagy-mediating factors, the bacteria are efficiently degraded. Figure created with BioRender.

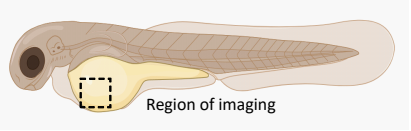
Region of imaging

A

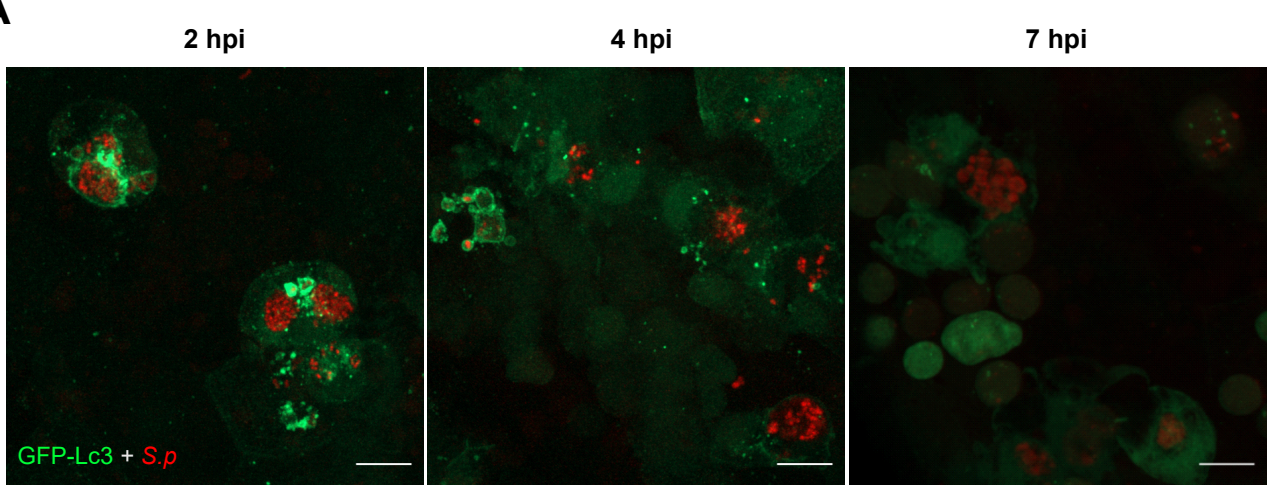
2 hpi
4 hpi
7 hpi
GFP-Lc3 + S.p

B

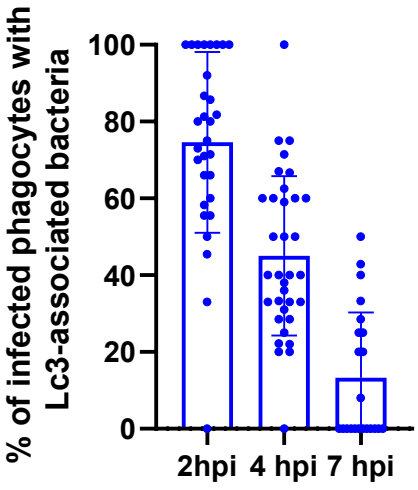
% of infected phagocytes with Lc3-associated bacteria
100
80
60
40
20
0
2hpi
4 hpi
7 hpi

C

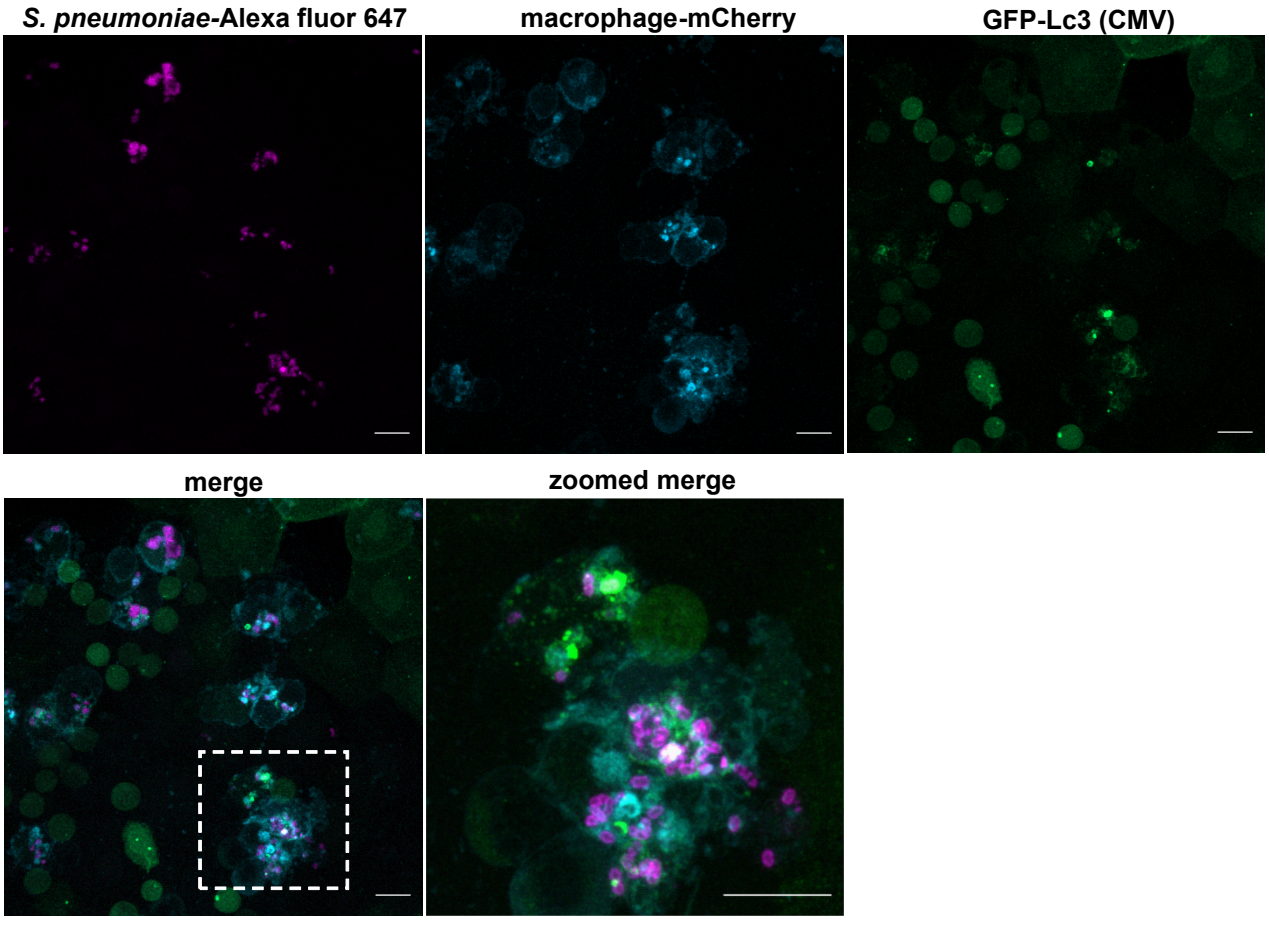
S. pneumoniae-Alexa fluor 647
macrophage-mCherry
GFP-Lc3 (CMV)
merge
zoomed merge

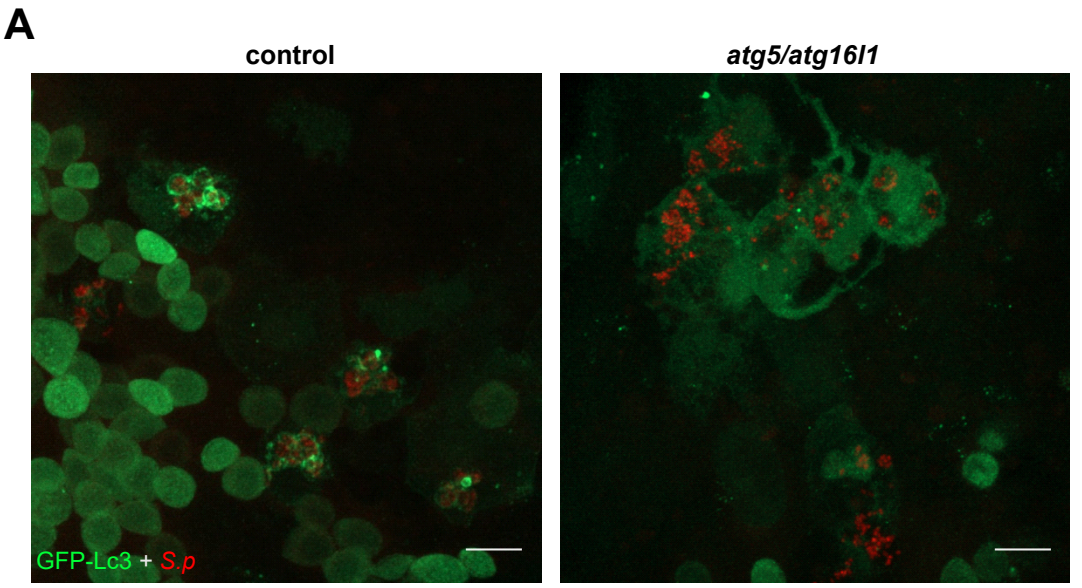
A
control
atg5/atg16l1
GFP-Lc3 + S.p

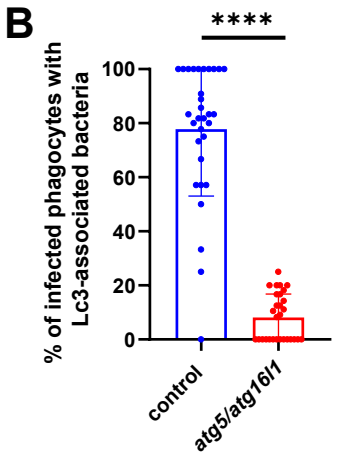
B
****
% of infected phagocytes with Lc3-associated bacteria
100
80
60
40
20
0
control
atg5/atg16l1

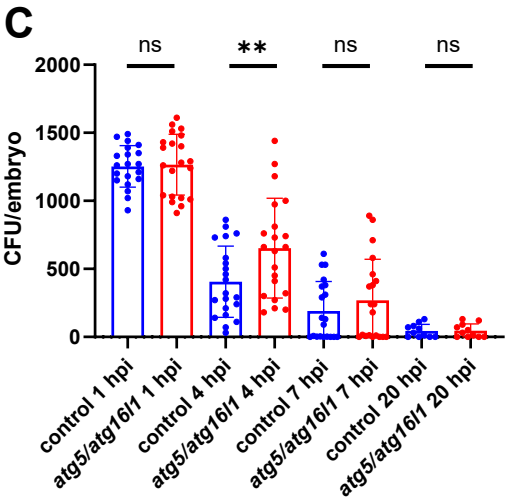
C
ns
**
ns
ns
CFU/embryo
2000
1500
1000
500
0
control 1 hpi
atg5/atg16l1 1 hpi
control 4 hpi
atg5/atg16l1 4 hpi
control 7 hpi
atg5/atg16l1 7 hpi
control 20 hpi
atg5/atg16l1 20 hpi

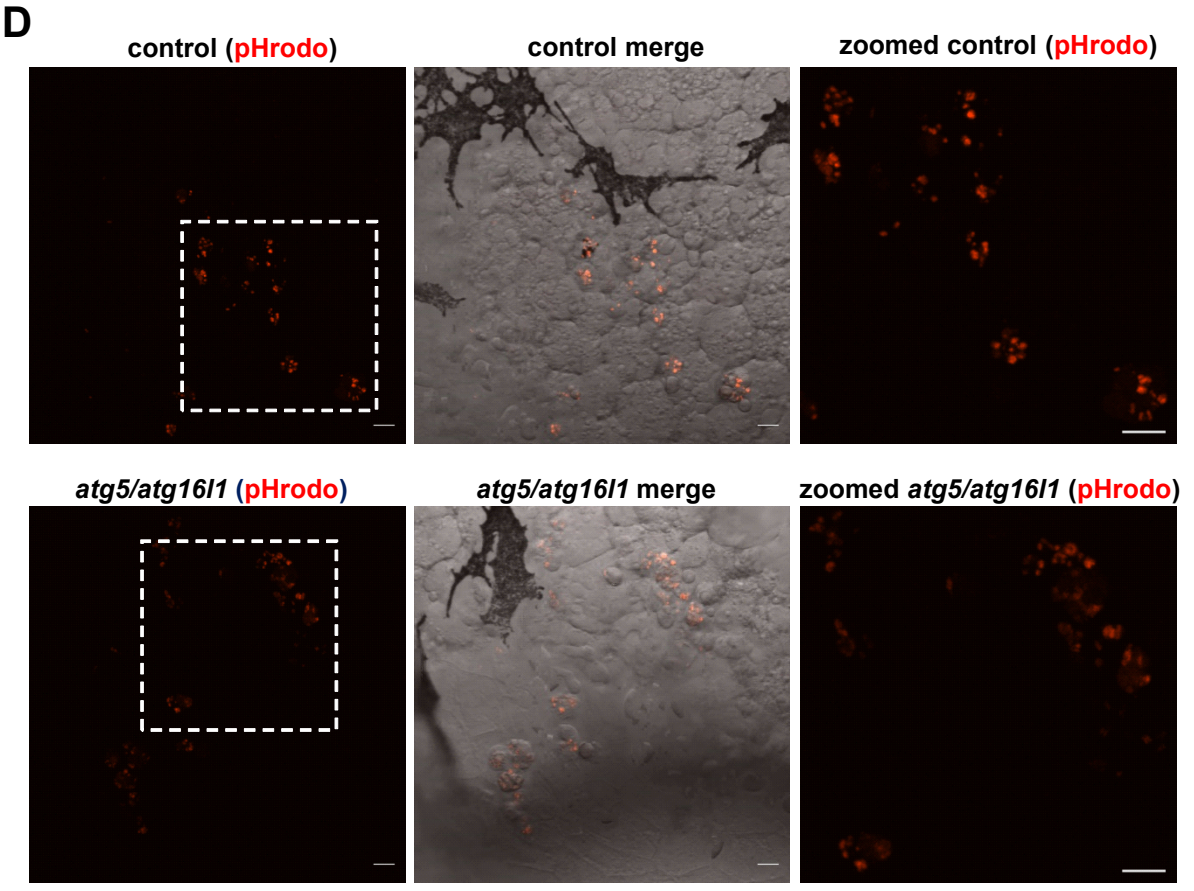
D
control (pHrodo)
control merge
zoomed control (pHrodo)
atg5/atg16l1 (pHrodo)
atg5/atg16l1 merge
zoomed atg5/atg16l1 (pHrodo)

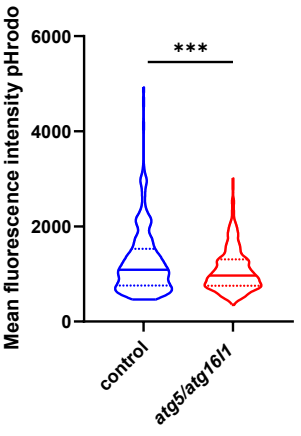
E
***
Mean fluorescence intensity pHrodo
6000
4000
2000
0
control
atg5/atg16l1

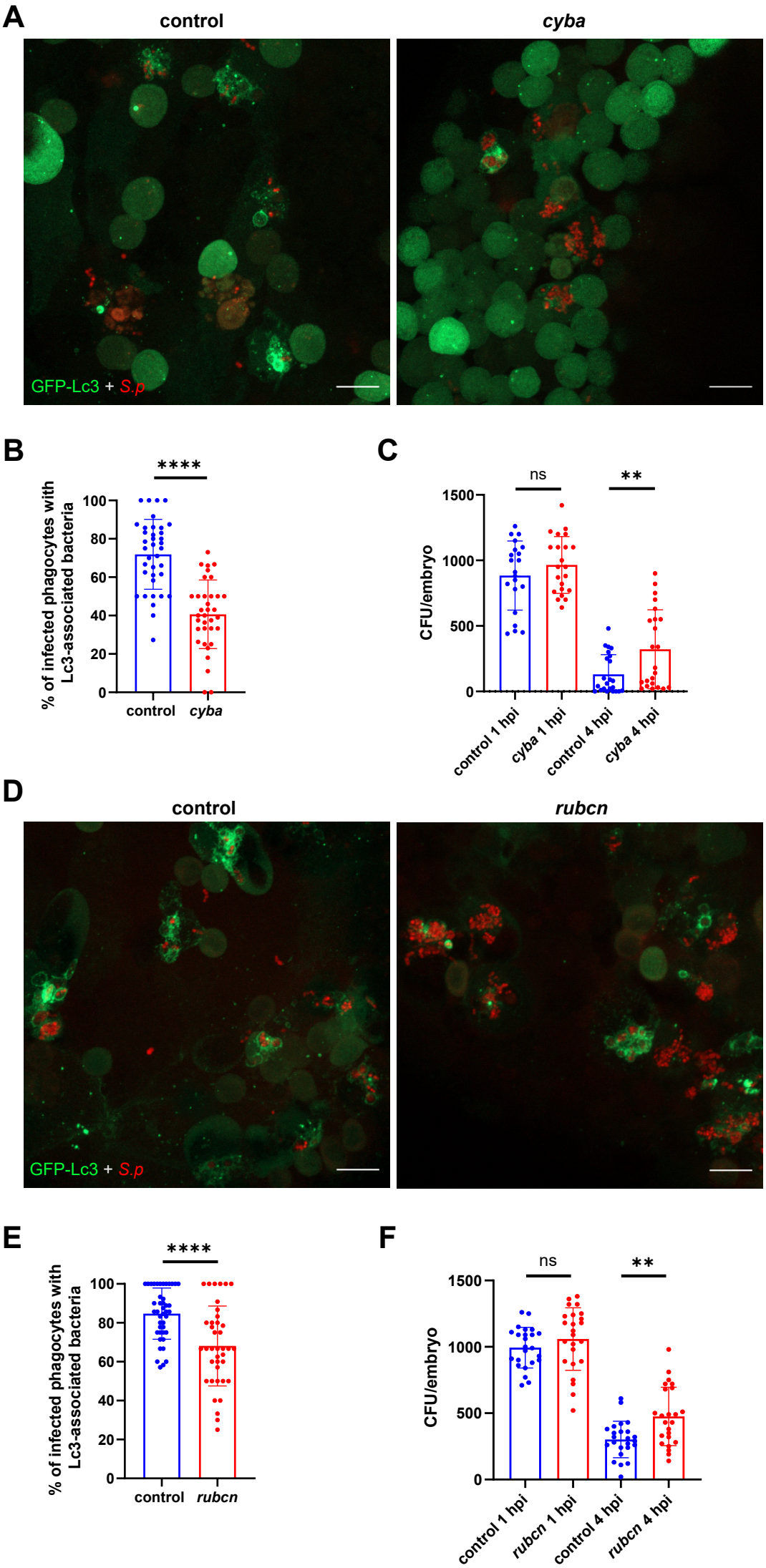
A
control
cyba
GFP-Lc3 + S.p
B
****
% of infected phagocytes with Lc3-associated bacteria
100
80
60
40
20
0
control
cyba
C
ns
**
CFU/embryo
1500
1000
500
0
control 1 hpi
cyba 1 hpi
control 4 hpi
cyba 4 hpi
D
control
rubcn
GFP-Lc3 + S.p
E
****
% of infected phagocytes with Lc3-associated bacteria
100
80
60
40
20
0
control
rubcn
F
ns
**
CFU/embryo
1500
1000
500
0
control 1 hpi
rubcn 1 hpi
control 4 hpi
rubcn 4 hpi

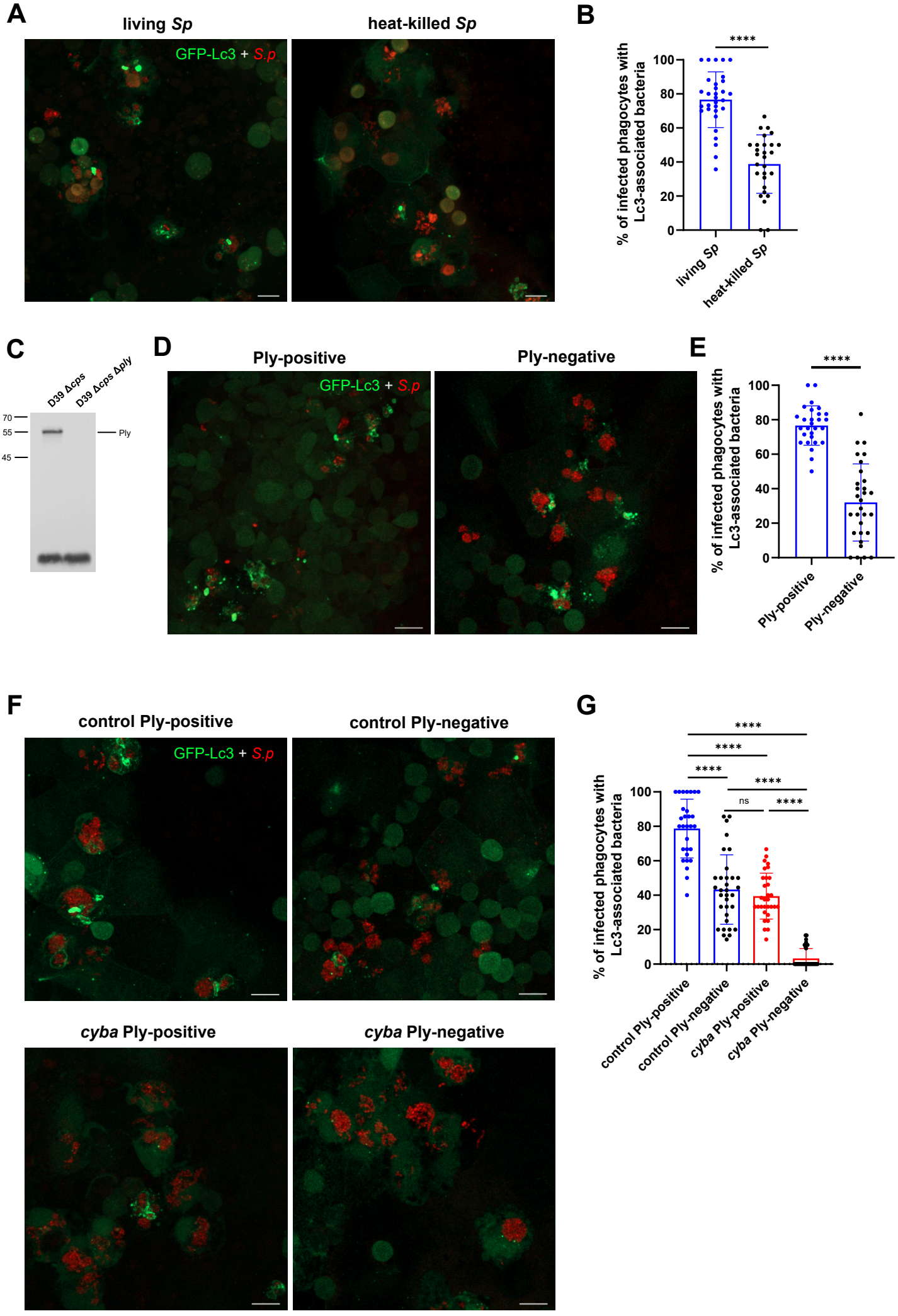
A
living Sp
heat-killed Sp
GFP-Lc3 + S.p
B
% of infected phagocytes with Lc3-associated bacteria
****
living Sp
heat-killed Sp
C
D39 Δcps
D39 Δcps Δply
70
55
45
Ply
D
Ply-positive
Ply-negative
GFP-Lc3 + S.p
E
% of infected phagocytes with Lc3-associated bacteria
****
Ply-positive
Ply-negative
F
control Ply-positive
control Ply-negative
GFP-Lc3 + S.p
cyba Ply-positive
cyba Ply-negative
G
% of infected phagocytes with Lc3-associated bacteria
****
ns
control Ply-positive
control Ply-negative
cyba Ply-positive
cyba Ply-negative

A

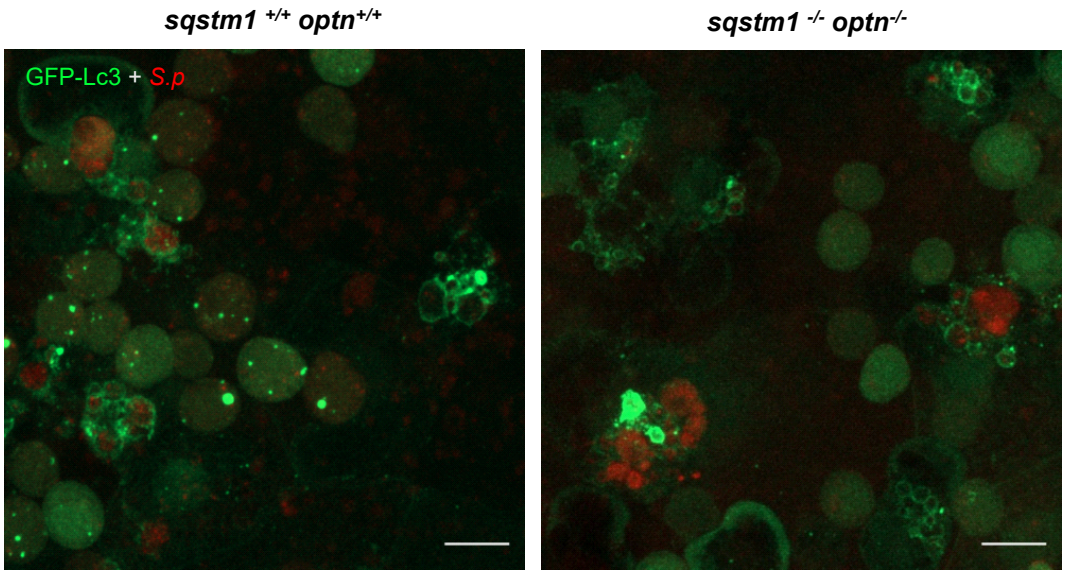
sqstm1 +/+ optn+/+
sqstm1 -/- optn-/-
GFP-Lc3 + S.p

B

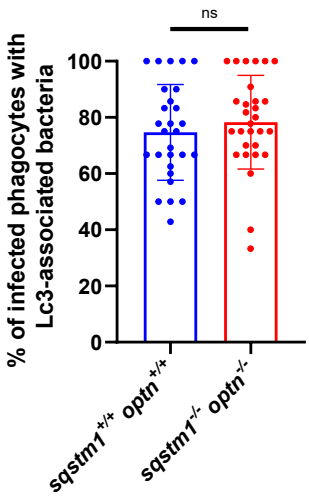
ns
% of infected phagocytes with Lc3-associated bacteria
100
80
60
40
20
0
sqstm1+/+ optn+/+
sqstm1-/- optn-/-

C

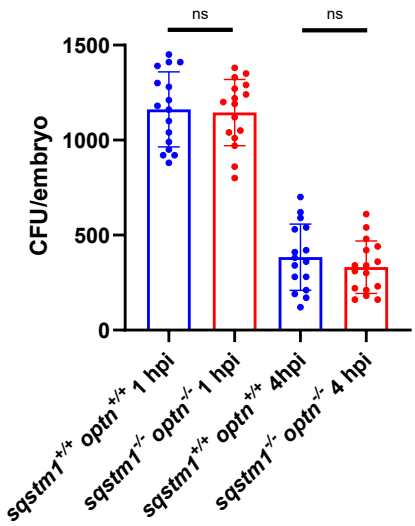
ns
ns
CFU/embryo
1500
1000
500
0
sqstm1+/+ optn+/+ 1 hpi
sqstm1-/- optn-/- 1 hpi
sqstm1+/+ optn+/+ 4hpi
sqstm1-/- optn-/- 4 hpi

D

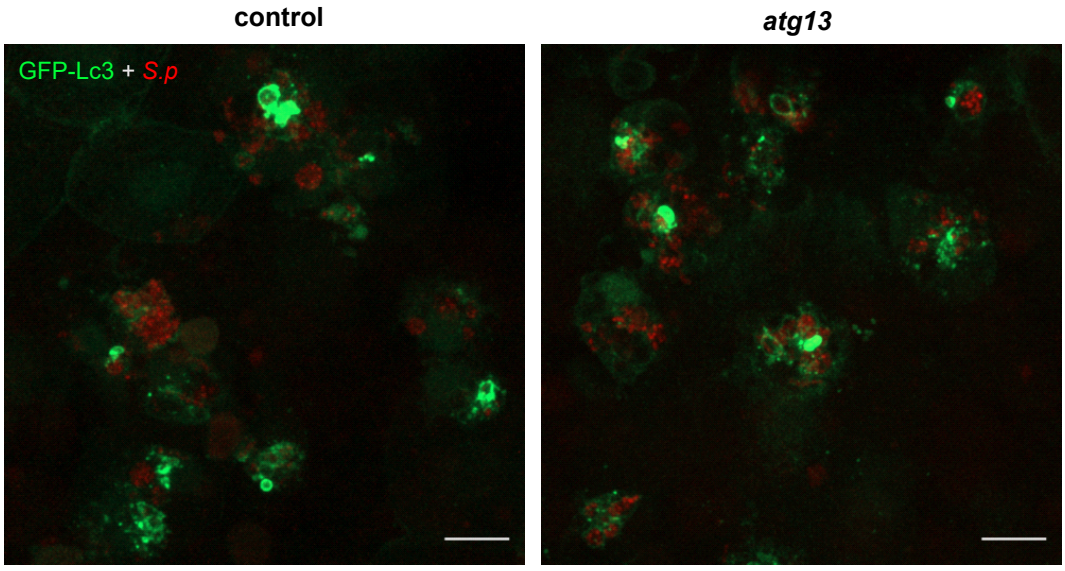
control
atg13
GFP-Lc3 + S.p

E

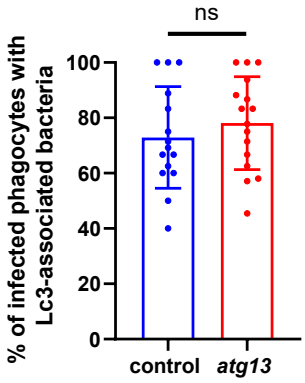
ns
% of infected phagocytes with Lc3-associated bacteria
100
80
60
40
20
0
control
atg13

A

PROTEIN	Alignment to *H.sapiens* TECPR1 (1164 aa)	AIR Domain Alignement	Protein Length
Tecpr1a (*D.rerio*)	78% Positives	95.5% Positives	1198 aa
Tecpr1b (*D.rerio*)	66% Positives	44.4% Positives	1105 aa

B

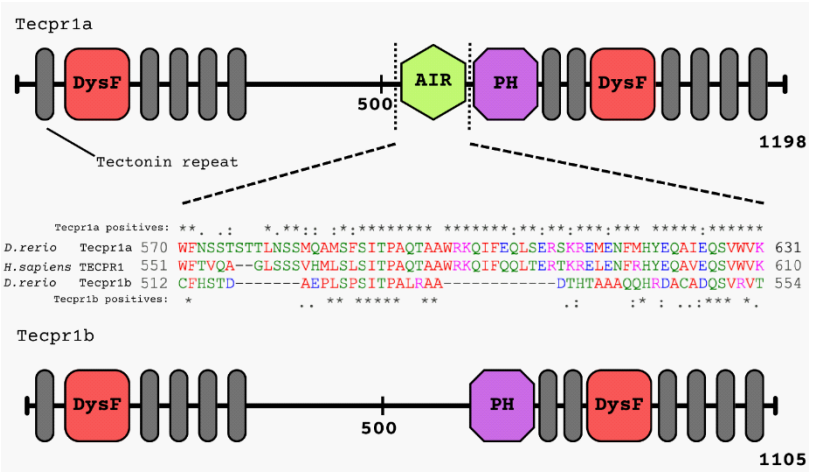

C

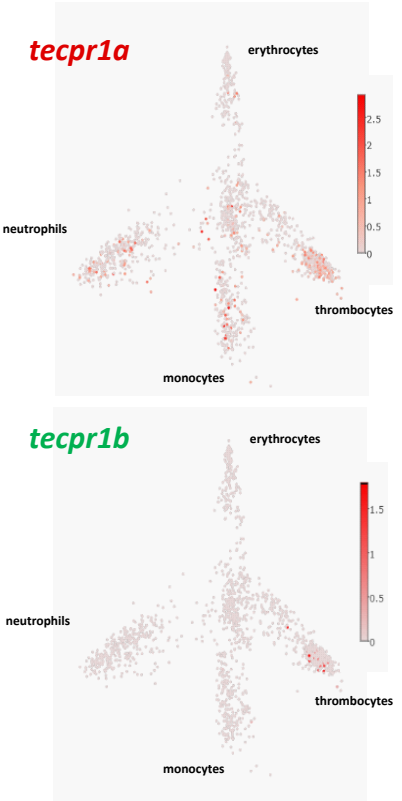

D

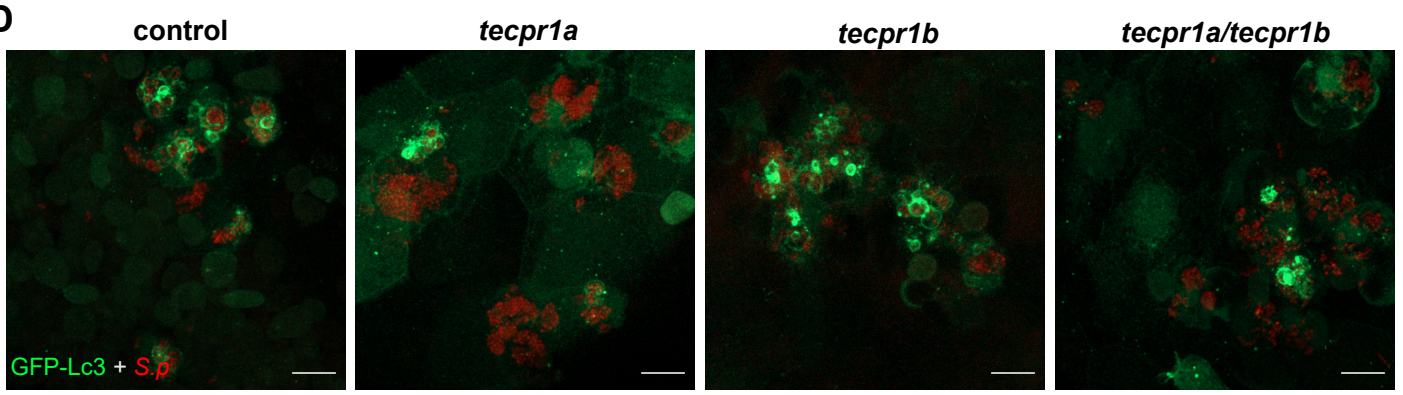

E

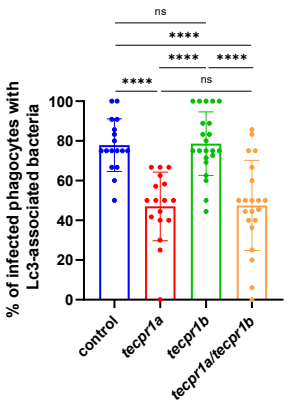

F

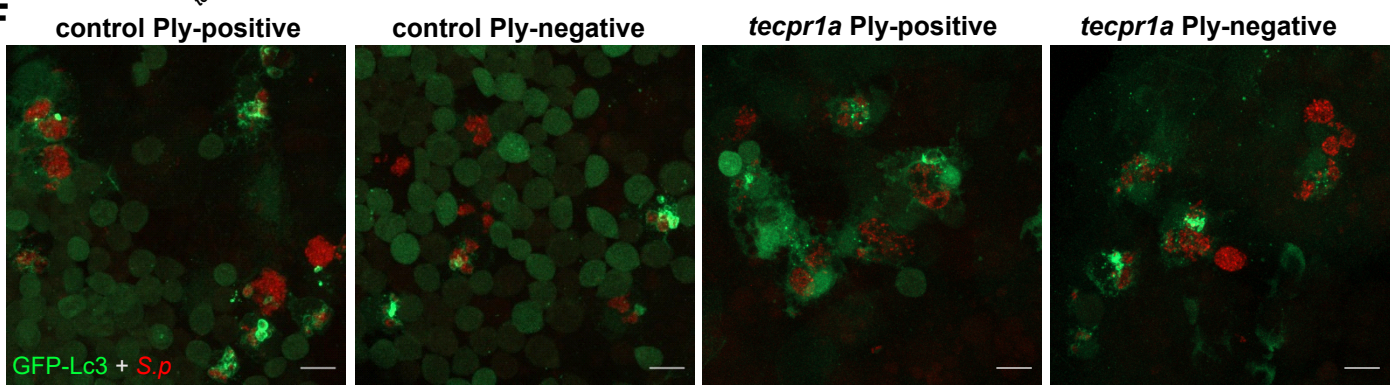

G

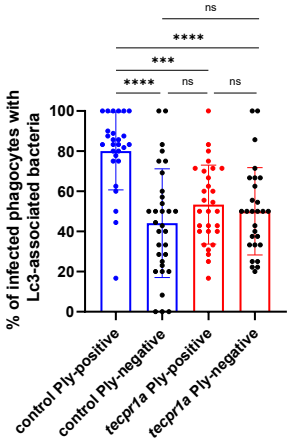

H

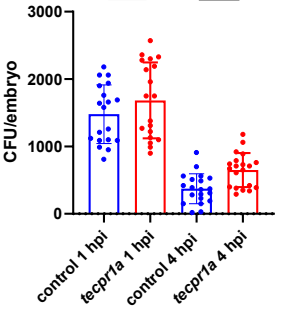

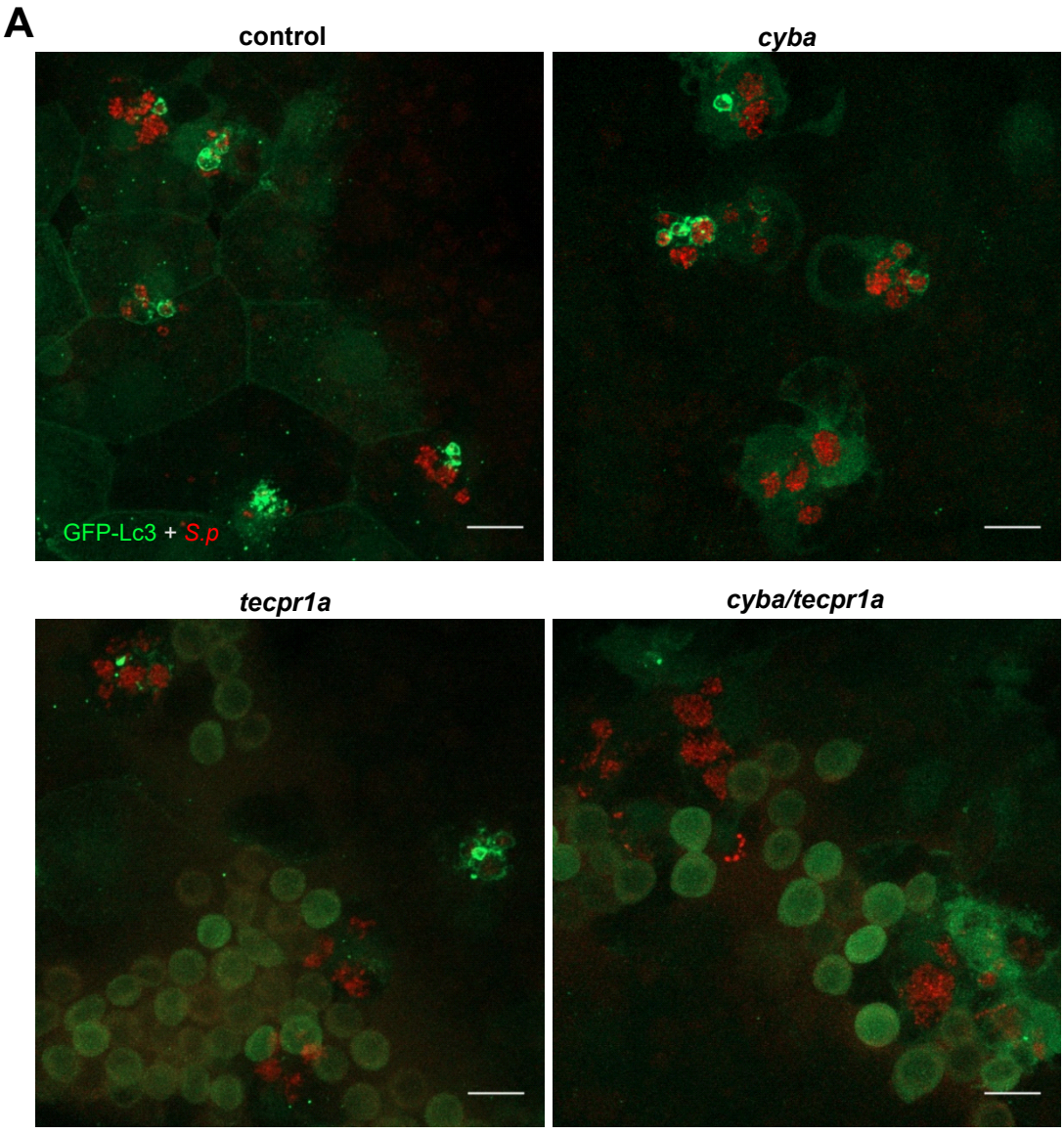
A
control
cyba
GFP-Lc3 + S.p
tecpr1a
cyba/tecpr1a

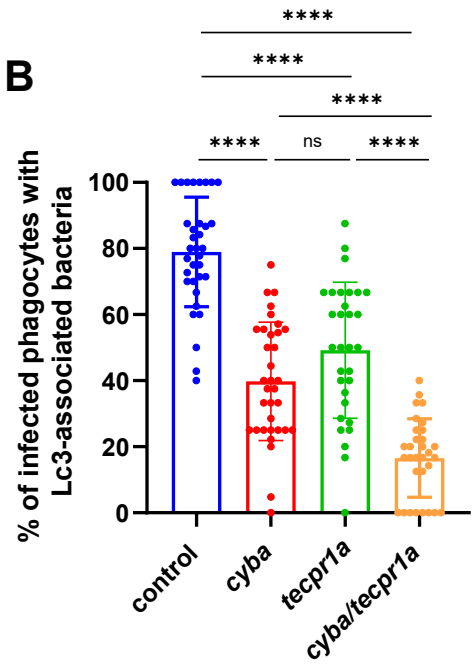
B
****
****
****
****
ns
****
% of infected phagocytes with Lc3-associated bacteria
100
80
60
40
20
0
control
cyba
tecpr1a
cyba/tecpr1a

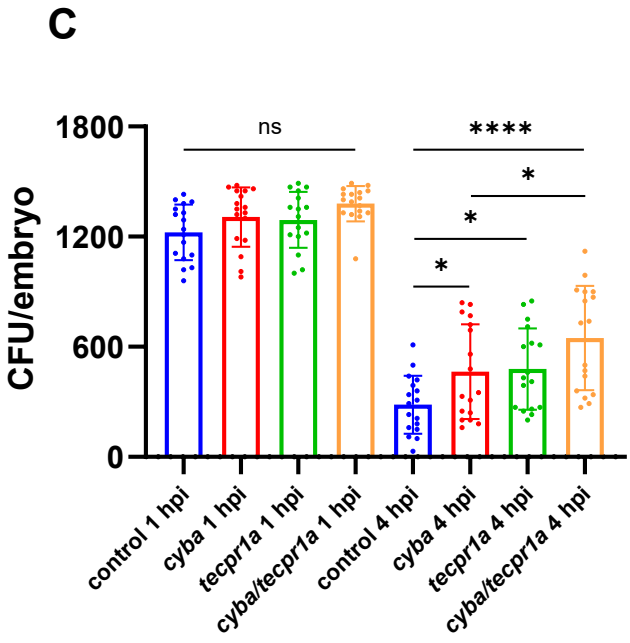
C
ns
****
*
*
*
CFU/embryo
1800
1200
600
0
control 1 hpi
cyba 1 hpi
tecpr1a 1 hpi
cyba/tecpr1a 1 hpi
control 4 hpi
cyba 4 hpi
tecpr1a 4 hpi
cyba/tecpr1a 4 hpi

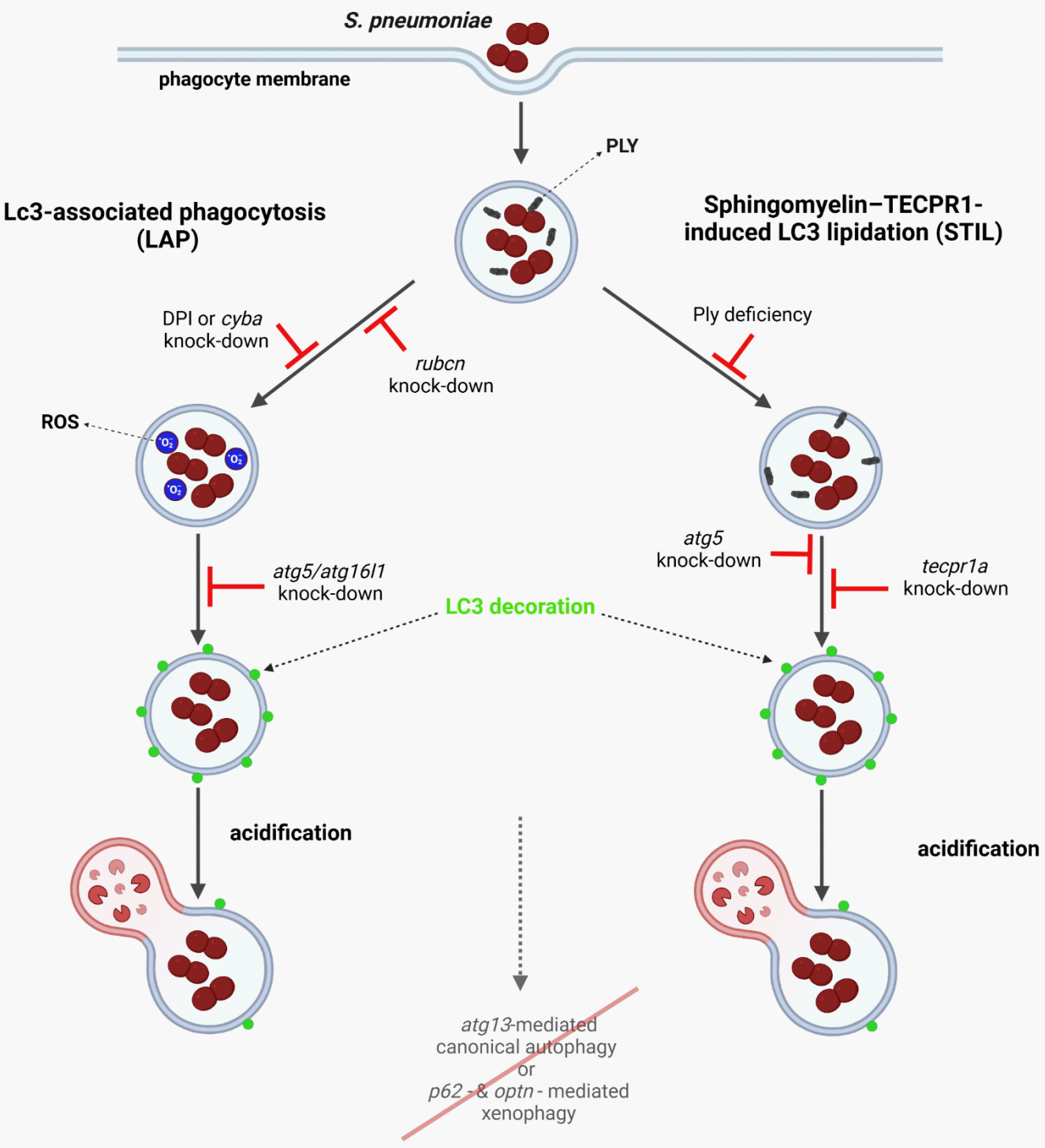
S. pneumoniae
phagocyte membrane
PLY
Lc3-associated phagocytosis (LAP)
Sphingomyelin–TECPR1-induced LC3 lipidation (STIL)
DPI or cyba knock-down
rubcn knock-down
Ply deficiency
ROS
atg5/atg16l1 knock-down
atg5 knock-down
tecpr1a knock-down
LC3 decoration
acidification
acidification
atg13-mediated canonical autophagy or p62 - & optn - mediated xenophagy